OPTIMUM SELECTION OF RENEWABLE ENERGY POWERED DESALINATION SYSTEMS

BY

Ahmad Hussain Al-Jabr

A Thesis Presented to the
DEANSHIP OF GRADUATE STUDIES

KING FAHD UNIVERSITY OF PETROLEUM & MINERALS

DHAHRAN, SAUDI ARABIA

In Partial Fulfillment of the
Requirements for the Degree of

MASTER OF SCIENCE

In

MECHANICAL ENGINEERING

May 2016

KING FAHD UNIVERSITY OF PETROLEUM & MINERALS

DHAHRAN- 31261, SAUDI ARABIA

DEANSHIP OF GRADUATE STUDIES

This thesis, written by **Ahmad Hussain Al-Jabr** under the direction his thesis advisor and approved by his thesis committee, has been presented and accepted by the Dean of Graduate Studies, in partial fulfillment of the requirements for the degree of **MASTER OF SCIENCE IN MECHANICAL ENGINEERING.**

Dr. Zuhair M. Gasem
Department Chairman

Dr. Salam A. Zummo
Dean of Graduate Studies

4/1/17
Date

Dr. Rached Ben-Mansour
(Advisor)

Dr. Mohammed A. Antar
(Member)

Dr. Syed A. M. Said
(Member)

2016

To my mother and father,

To my brothers and sisters,

To my wife and daughter

ACKNOWLEDGMENTS

I am most grateful to Almighty ALLAH, the compassionate, the merciful, for giving me health, power and patience to complete this work. Peace and blessings of ALLAH be upon his last messenger Mohammed and his progeny.

Thereafter, acknowledgement is due to King Fahd University of Petroleum and Minerals and to Mechanical Engineering Department for supporting my research work.

I wish to express my deep appreciation and gratitude to Dr. Rached Ben-Mansour, my thesis advisor, for the encouragement, valuable time and continuous guidance given by him. I also wish to thank my committee members, Dr. Mohammed A. Antar and Dr. Syed A. M. Said for their guidance and constructive comments. I would like also to acknowledge Dr. Zuhair M. Gasem, Chairman of Mechanical Engineering Department, and Dr. Salam A. Zummo, Dean of Graduate Studies, for their support and encouragement. I wish also to thank all faculty members of Mechanical Engineering Department for their assistance and advices.

My heartfelt thanks and appreciation are due to my patents, brothers, sisters, friends and colleagues for their encouragement and prayers. Special thanks are due to my wife and daughter “Fatemah” for their patience and support.

TABLE OF CONTENTS

LIST OF TABLES

LIST OF FIGURES

LIST OF ABBREVIATIONS

ED	:	Electro-dialysis
EE	:	Energy Excess
HDH	:	Humidification-Dehumidification desalination
MED	:	Multi-Effect Desalination
MSF	:	Multi-Stage Flashing
MVC	:	Mechanical Vapor Compression
N	:	Number of
P	:	Power
PV	:	Photovoltaic
REDS	:	Renewable Energy Desalination Systems
RO	:	Reverse Osmosis
Tank	:	Water volume in the storage tank
TVC	:	Thermal Vapor Compression
VC	:	Vapor Compression

Subscripts

avg	:	average

d	:	distillate
i	:	number of the month
n	:	needed

ABSTRACT

Full Name : Ahmad Hussain AlJabr

Thesis Title : Optimum Selection of Renewable Energy Powered Desalination Systems

Major Field : Mechanical Engineering

Date of Degree : May 2016

Research and development of desalination technologies are becoming highly important because of the rapid increase in fresh water demand. Researchers are continually working on improving the existing desalination technologies and exploring new methods and ideas to desalinate salty water. The main goal is to come up with cost-effective systems. Renewable energy desalination is becoming nowadays an attractive option because of its viability of producing fresh water, technology improvement continuation, limitation of conventional sources and compatibility between water needs and renewable resources availability. More importantly, using renewable energy to power desalination systems is extremely important for reducing global emissions and protecting the environment. Comparison between different renewable powered desalination technologies were mainly based on different system capacity, energy source system, feed-water salinity and system components. This makes the economical comparison almost impossible. There is an existing gap in having an economical comparison to different renewable energy powered desalination systems with the same basics such as availability of renewable and water resources.

This research is an attempt to provide a systematic methodology to obtain the most cost-effective renewable energy powered desalination system given the capacity required and the resources of a given location. Different combinations are compared. Results show that for Dhahran cost of water produced by RO-Wind is 1.366 $/m^3 to 1.273 $/m^3 and by RO-PV is 2.119 $/m^3 to 1.983 $/m^3 and by MED-solar is 2.282 $/m^3 to 2.026 $/m^3 for system capacity of 1000 m^3 to 10,000 m^3, respectively. For Dhahran, RO-Wind is the optimum selection. Results for different cities across the kingdom show that the optimum location for implementing RO-Wind is Dhahran while the optimum locations for RO-PV and MED-Solar are Jeddah and Yanbu.

ملخص الرسالة ABSTRACT (In Arabic)

الاسم الكامل : أحمد حسين الجبر

عنوان الرسالة : الاختيار الأمثل لأنظمة تحلية المياه المشغلة باستخدام الطاقة المتجددة

التخصص : الهندسة الميكانيكية

تاريخ الدرجة العلمية : رجب 1437 هـ

عمليات البحث والتطوير لأنظمة تحلية المياه تكتسب أهمية عالية نظراً للزيادة المطردة في الحاجة للمياه العذبة. يعمل الباحثون بشكل متواصل على تطوير الأنظمة القائمة واكتشاف طرق وأفكار جديدة لتحلية المياه المالحة. الهدف الرئيسي هو الوصول لأنظمة ذات تكلفة منخفضة. تحلية المياه بواسطة الطاقة المتجددة أصبحت اليوم خيار جذاب بسبب قدرتها على إنتاج المياه المحلاة والتطوير المستمر لهذه التقنيات ومحدودية مصادر الطاقة التقليدية بالإضافة للتوافق بين الحاجة للماء وتوفر مصادر الطاقة المتجددة. أيضا، استخدام الطاقة المتجددة لتشغيل أنظمة التحلية مهم للغاية للتقليل من الانبعاث الحراري وحماية البيئة. المقارنة بين مختلف هذه الأنظمة مبنية بشكل أساسي على اختلاف في السعة ومصدر الطاقة وملوحة المياه وأجزاء النظام المختلفة. هذا الاختلاف يجعل المقارنة الاقتصادية بين مختلف الأنظمة شبه مستحيلة. هناك فجوة في المقارنة الاقتصادية بين مختلف أنظمة تحلية المياه المشغلة بواسطة أنظمة الطاقة المتجددة بناءً على نفس الأسس مثل تواجد مصادر الطاقة المتجددة والمياه.

هذا البحث هو محاولة لتوفير منهجية للحصول على النظام الأقل تكلفة اقتصادية بإعطاء السعة المطلوبة وبيانات الطاقة المتجددة لمكانٍ ما. في هذه الرسالة تم مقارنة أنظمة مختلفة تشمل التناضح العكسي-طاقة الرياح، التناضح العكسي-الألواح الشمسية والتقطير متعدد المراحل-الطاقة الشمسية الحرارية. النتائج لمدينة الظهران –المملكة العربية السعودية- تبين أن تكلفة إنتاج الماء باستخدام التناضح العكسي-طاقة الرياح هو 1.366 دولار لكل متر مكعب ($/م^3) إلى 1.273 ($/م^3) وباستخدام التناضح العكسي-الألواح الشمسية هو 2.119 ($/م^3) إلى 2.048 ($/م^3) وباستخدام التقطير متعدد المراحل-الطاقة الشمسية الحرارية هو 2.282 ($/م^3) إلى 2.026 ($/م^3) لنظام سعته 1000 م^3 إلى 10000 م^3، على التوالي. للظهران، التناضح العكسي-طاقة الرياح هو الخيار الأمثل. النتائج لمجموعة من المدن

في المملكة العربية السعودية تبين أن أفضل مدينة لتطبيق نظام التناضح العكسي-طاقة الرياح هي الظهران بينما جدة وينبع هما الخيار الأمثل لتطبيق التناضح العكسي-الألواح الشمسية وكذلك التقطير متعدد المراحل-الطاقة الشمسية الحرارية.

CHAPTER 1

INTRODUCTION

Water is a critically important element in mankind's life. However, Water demand is rapidly increasing because of the population increase and uncontrolled human and industrial usage. Eight and a half billion gallons/day of water is desalinated over the world (Al-Karaghouli, et al., 2009). This number is expected to increase in the near future because of continues increase of population and industry. Desalination is recognized as energy intensive process where 50% of the total cost of desalination is energy cost.

Increasing of conventional fossil fuels costs, conventional resources being depleted, its environmental effects lead people to think in other power alternatives. On the other side, renewable energy is abundant on earth, available, sustainable, free and environmentally friendly. People are working in utilizing this energy in producing power and water. Utilization of renewable energy in purifying water is becoming more attractive nowadays. The main concern is the optimum economical selection of renewable energy powered desalination.

Existing comparisons between different desalination technologies and specifically renewable powered desalination technologies were mainly based on different system

capacity, energy source system, feed-water salinity and system components. This makes the economical comparison almost impossible. There is an existing gap in having an economical comparison of different renewable powered desalination systems with the same basics such as availability of renewable and water resources. This research is an attempt to provide a computerized tool to evaluate the specific cost and compare between cost-effective energy-efficient renewable energy powered desalination systems for the same conditions including capacity, feed salinity and renewable resources.

In order to understand the different desalination technologies and renewable energy technologies, a brief description of each system is presented. In the following sections, general overviews on desalination systems, renewable power systems and local (Saudi Arabia, Dhahran) renewable resources and renewable energy powered desalination systems.

1.1 Desalination systems

Desalination is the process of separation of salts from salty water to produce fresh water. Desalination systems are classified as distillation process –or thermal- and membrane process. Distillation is the process where feed water is heated till fresh water evaporates then condenses and collected and it includes Multi-stage flashing (MSF), Multi-effect desalination (MED), Vapor compression (VC) and others. Membrane is filtration process and it includes mainly reverse osmosis (RO) and

Electrodialysis (ED). Table 1 shows the worldwide breakdown of desalination system capacity.

One of the significant differences between the two processes is that energy consumption is independent of salt concentration in distillation. However, it is highly dependent in membrane processes (Al-Karaghouli & Kazmerski, 2013). This is the reason behind using membrane desalination, RO mainly, for brackish water.

Table 1: Worldwide breakdown of Desalination capacity share (Al-Karaghouli, et al., 2009)

Membrane process	Percentage	Distillation process	Percentage
RO	44	MSF	40
ED	6	MED	4
		VC	3
New-concept process			3

1.1.1 Distillation

Distillation process is simulating the water cycle in nature where salty water is heated, partially evaporated and then condensed producing fresh water. This category includes MSF, MED and VC. One of the disadvantages in these systems is that it requires both thermal energy to heat the feed water and electrical energy to operate system's pumps. Usage of low-cost thermal energy available in the exhaust of steam turbine, for example, effectively reduces desalination production cost.

Multi-stage flashing (MSF) distillation is represented in Figure 1. In MSF, feed-water is heated and pressurized and enters a chamber at pressure slightly lower than water saturation vapor pressure. Small fraction of water flashes into steam and steam is condensed and collected where condensation latent heat is utilized in preheating the feed-water.

Multi-Effect distillation (MED), also named in some literature as multi-effect evaporation (MEE) or multi-effect boiling (MEB), is represented in Figure 2. In MED, feed-water is spread over heat exchanger tubes, which are heated by external source, to elevate its temperature. Fraction of the feed-water is evaporated and then sent to the next stage, which is at slightly lower pressure, acting as heat source to heat and evaporate the remaining feed-water while it condensed and collected as fresh water.

Vapor compression (VC) distillation is represented in Figure 3. In VC, vapor is compressed either mechanically (MVC) or thermally (TVC) to increase its pressure. Vapor is then sent to heat exchanger tubes where feed-water is spread over its outer surface to be heated, evaporated and sent to the compressor for process continuation. Feed water is preheated utilizing the heat of fresh water condensation.

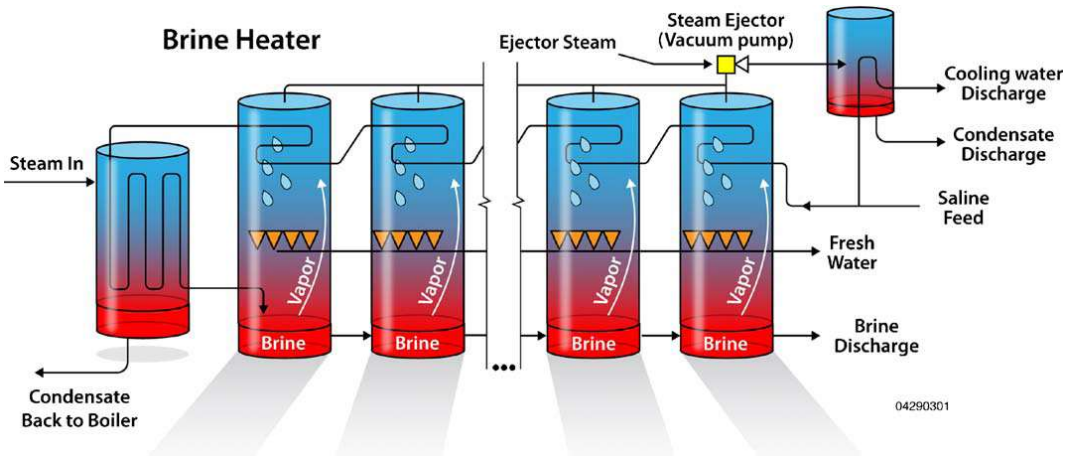

Figure 1: MSF distillation diagram (Al-Karaghouli, et al., 2009)

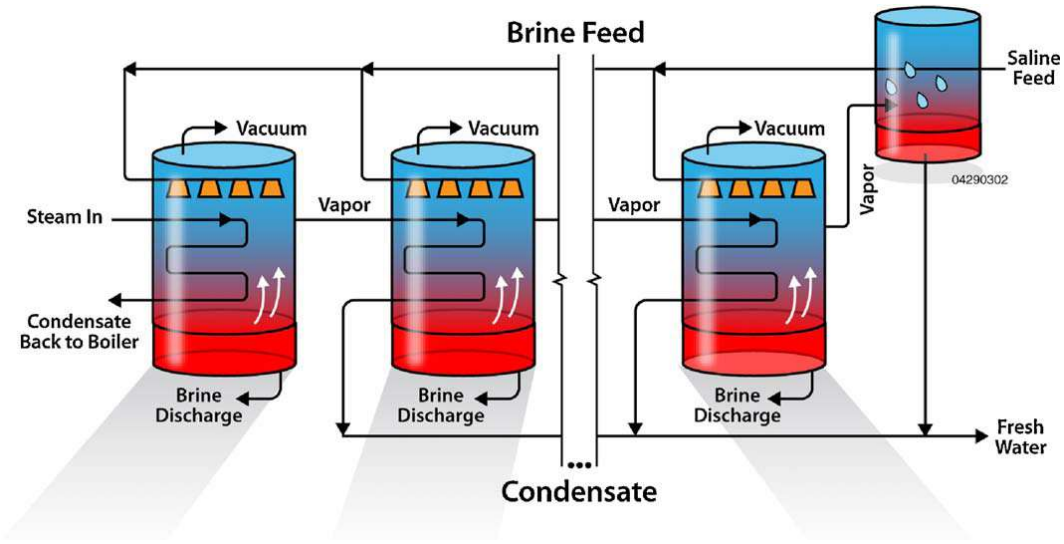

Figure 2: MEE diagram (Al-Karaghouli, et al., 2009)

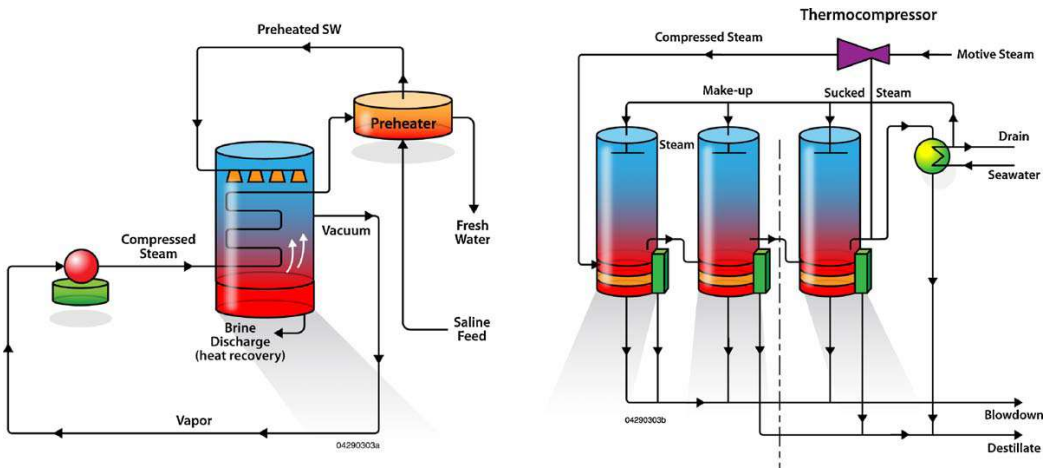

Figure 3: Diagrams of Vapor Compression (VC); left: Mechanical (MVC) and right: Thermal (TVC) (Al-Karaghouli, et al., 2009)

1.1.2 Membrane

Membranes mimic the process of salt separation available in human body (Al-Karaghouli, et al., 2009). Membrane category includes reverse osmosis (RO) and electrodialysis (ED). Unlike distillation processes, membrane processes require only electricity.

Reverse Osmosis (RO) desalination is represented in Figure 4. In RO, feed-water is pressurized and pumped against the membrane where salts are separated from saline solution. Applied pressure should overcome the osmotic pressure developed in the saline solution. As a result of purifying some water, osmotic pressure does increase which means higher pressure should be applied. To optimize the operating pressure, some of the feed-water, now called brine, has to be discharged.

Electrodialysis desalination (ED) is presented in Figure 5. In ED, direct electrical current is used to selectively move salt ions through selective permeable membranes where positive salt ions move to the negative electrodes and negative salt ions move to the positive electrodes producing fresh water.

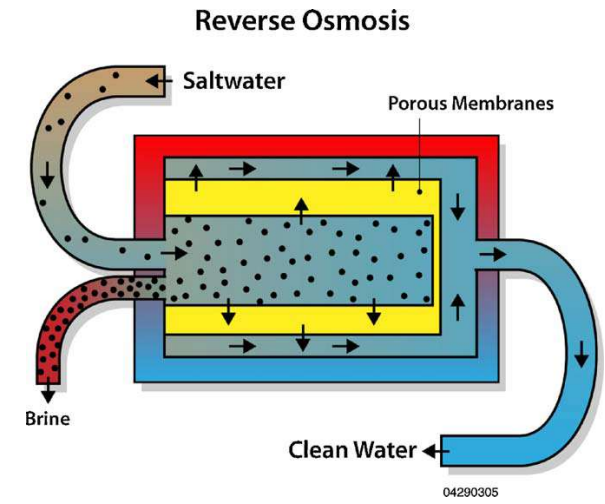

Figure 4: Diagram of RO desalination (Al-Karaghouli, et al., 2009)

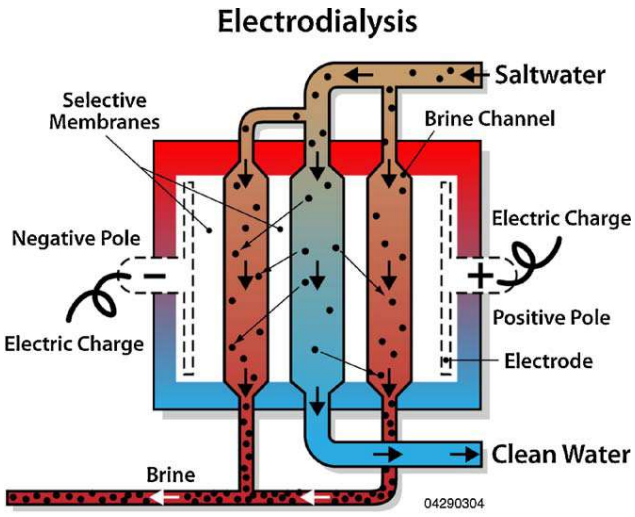

Figure 5: Diagram of Electrodialysis (Al-Karaghouli, et al., 2009)

1.2 Renewable energy systems

Renewable energy is the energy which comes from natural resources such as sunlight, wind, rain, tides, and geothermal heat. Unlike fossil fuels, renewable energy are sustainable, available everywhere (depend upon type of energy), environmental friendly. Utilizing renewable energy sources has the advantages of reducing global warming and CO_2 emissions. Renewable energy is classified based on energy source into:

- Hydropower
- Wind power
- Solar Photovoltaic (PV)
- Solar thermal
- Geothermal power
- Ocean power

Saudi Arabia has abundant solar radiation because of its geological location and average wind speeds. Investigations on the feasibility of applying hybrid solar PV-wind energy systems at Dhahran, Saudi Arabia were presented (Elhadidy & Shaahid, 1999). They conclude that Dhahran has very high potential of applying such renewable systems. Because of that, more focus is given to solar and wind power.

1.2.1 Solar thermal and Solar Photovoltaics (PV)

Sun is radiating heat and light. Solar thermal energy is utilizing the heat from the sun whereas solar photovoltaics utilizing the light. Table 2 shows the monthly average daily solar radiation on Dhahran, Saudi Arabia (Elhadidy & Shaahid, 2007). These numbers are averaged over the years of 1986-1993 and the overall yearly average daily radiation in Dhahran is 8.84 kWh/m^2.

Table 2: Monthly average daily global solar radiation at Dhahran, Saudi Arabia (Shaahid & Elhadidy, 2003)

Month	Global Solar Radiation (Wh/m^2)
January	3790
February	4612
March	5430
April	6456
May	7323
June	7960
July	7559
August	7160
September	6512
October	5378

November	4273
December	3615
AVG	5837

Figure 6 shows the monthly average solar radiation at Dhahran for the years [1986-1993]. It is easily indicated that solar radiation is almost in a repetition cycle over the year.

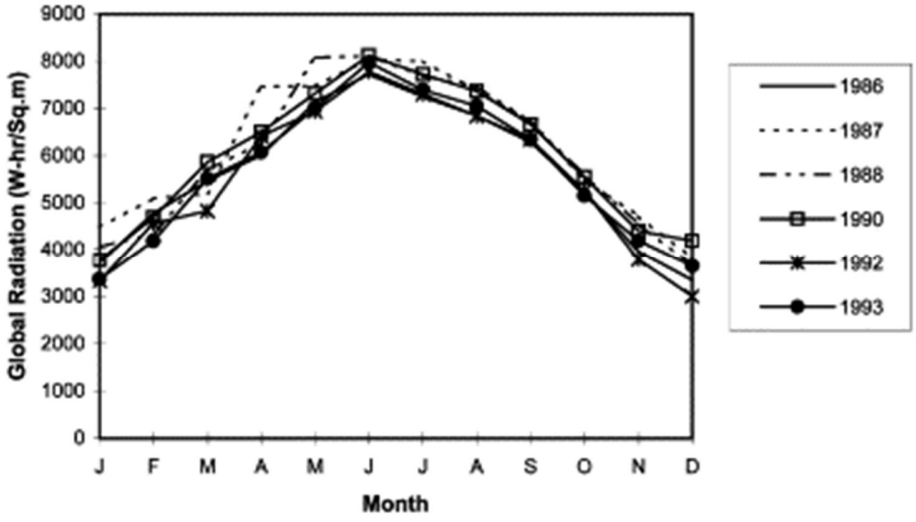

Figure 6: Monthly average daily global radiation at Dhahran (Shaahid & Elhadidy, 2003)

1.2.2 Wind Turbines

Unlike solar radiation, wind speed does not follow clear pattern and it is in continues change. This can be seen clearly in Figure 7. Figure 8 shows the monthly average wind speed over the years 1986 to 1997. Figure 9 shows the yearly average wind speed of Dhahran over the same period. Even the yearly average wind speed is fluctuating and maximum percentage change of more than 50% between year 1990 and year 1996 is observed. The overall average wind speed at Dhahran is 5.2 m/s (Elhadidy & Shaahid, 2007).

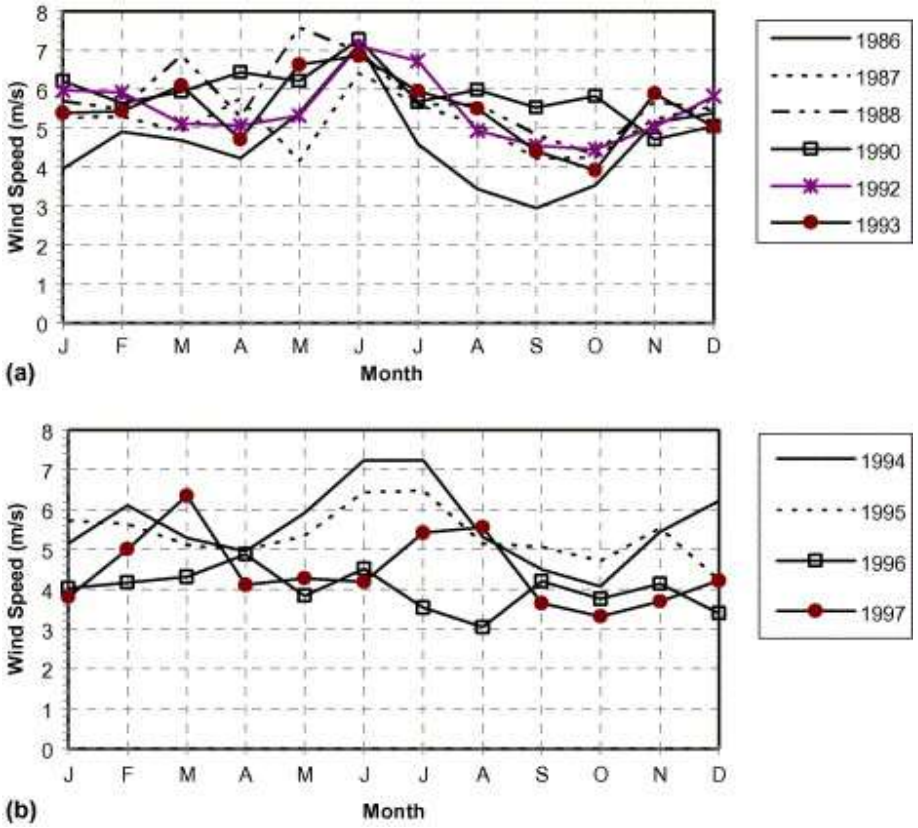

Figure 7: (a) Monthly avg. wind speed at Dhahran (1986–1993); (b) Monthly avg. wind speed at Dhahran (1994–1997). (Elhadidy & Shaahid, 2005)

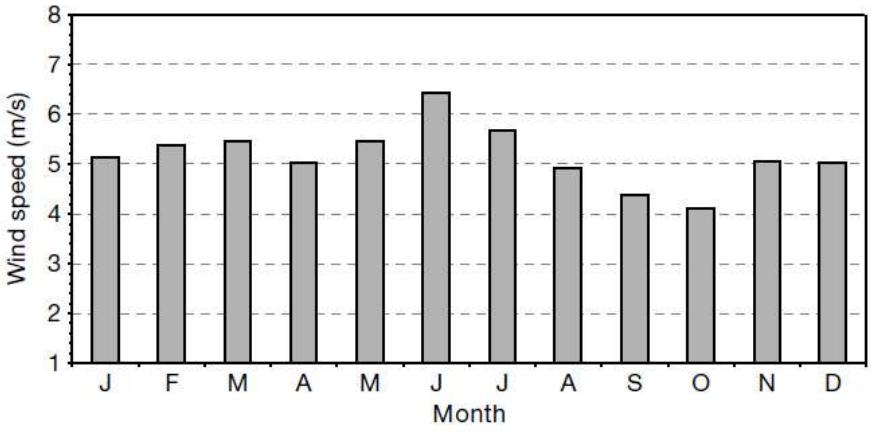

Figure 8: Monthly avg. wind speed at Dhahran (avg. of the period 1986–1997)

(Elhadidy & Shaahid, 2007)

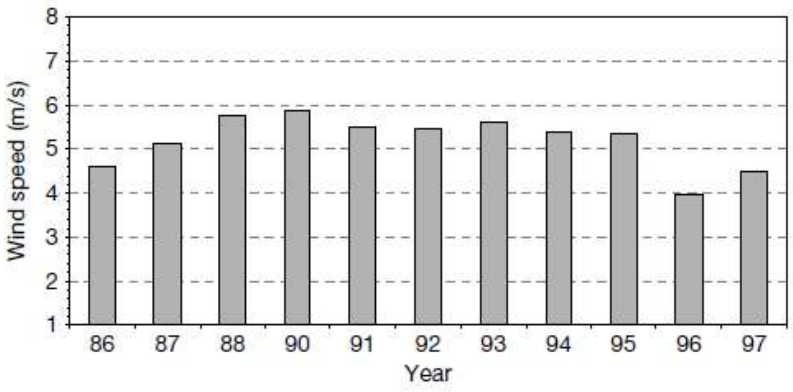

Figure 9: Yearly average wind speeds at Dhahran (Elhadidy & Shaahid, 2007)

1.3 Renewable Energy Powered Desalination systems (REDS)

Renewable energy desalination is becoming nowadays an attractive option because it proves its viability of producing fresh water, technology improvement continuation, limitation of conventional sources and compatibility between water needs and renewable resources availability. The systems could be classified into direct and indirect systems. Direct systems are stand-alone renewable desalination systems, whereas indirect have two coupled renewable-power and conventional-desalination technologies.

1.3.1 Direct REDS

Direct REDS are stand-alone systems where mainly solar thermal energy is used to heat, evaporate salty water which then condensed and collected. Solar still and humidification-dehumidification are considered direct REDS. Solar stills, in general, have low efficiency below 45% and very small capacity of 4-6 L per m^2 per day (Al-Karaghouli, et al., 2009). Figure 10 shows three types of solar stills: multiple-tray tilted still, concentrated mirror still and tilted wick still. Humidification-dehumidification (HDH) is the process where brine water is heated and used to heat and humid air stream, air then cooled and fresh water is condensed and collected. Figure 11 shows HDH processes with two schemes: open-water closed-air cycle and open-air closed-water cycle.

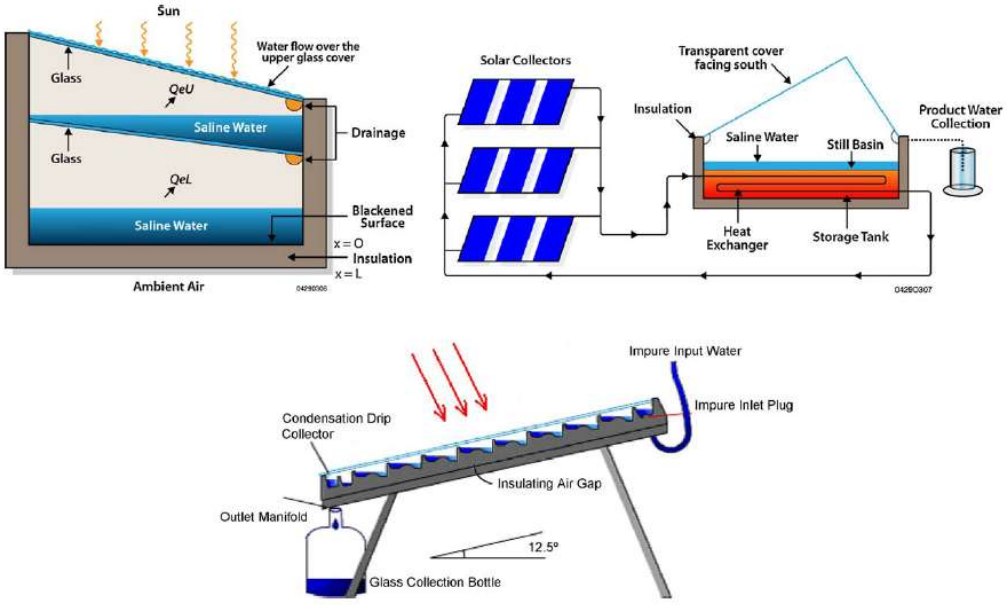

Figure 10: Different Solar Still Schematics (Al-Karaghouli, et al., 2009)

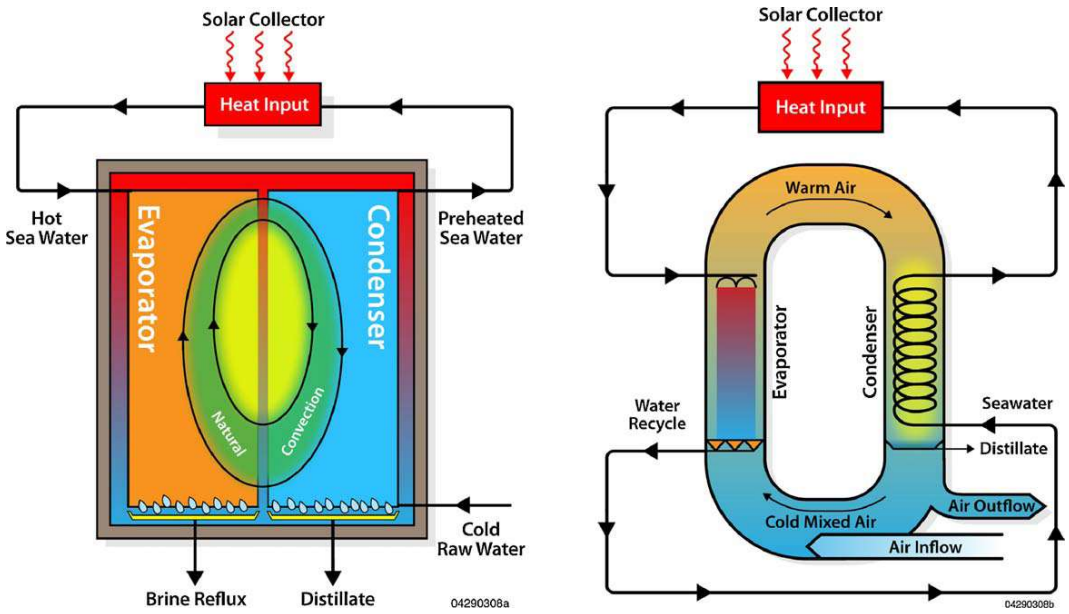

Figure 11: Schematics of HDH desalination. Left: open-water closed-air cycle and Right: open-air closed-water cycle (Al-Karaghouli, et al., 2009)

1.3.2 Indirect REDS

Indirect REDS are systems that composed of two stand-alone systems; renewable energy and conventional desalination. Figure 12 shows the possible combinations between renewable power technologies and desalination technologies. However, proper matching should be carefully investigated to end up with a rigid system that provides water at reasonable cost. Table 3 shows the most promising combinations of REDS.

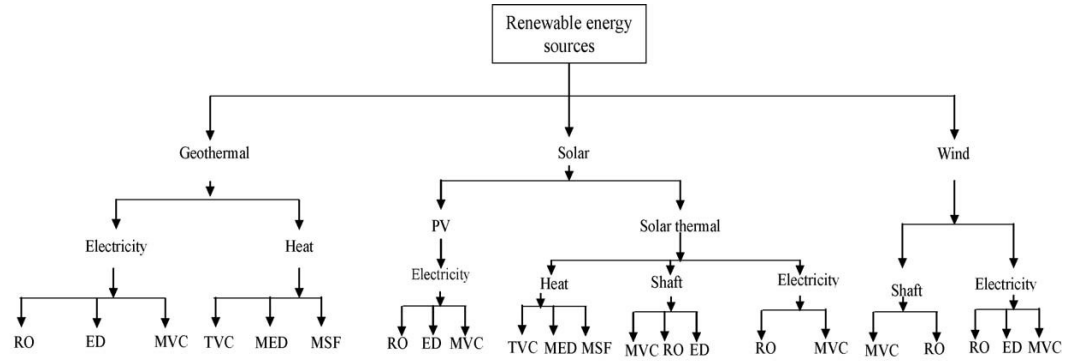

PV= Photovoltaic, RO= Reverse osmosis, ED= Electrodialysis, MVC= Mechanical vapor compression, MED= Multi effect distillation, MSF= Multi stage flash distillation, TVC= Thermal vapor compression

Figure 12: Possible REDS combinations (Eltawil, et al., 2009)

Table 3: Most Promising REDS combinations (Al-Karaghouli, et al., 2009)

Renewable Energy	Desalination Process				
	MSF	MED	VC	RO	ED
Wind			✓	✓	
Solar Photovoltaic				✓	✓
Solar Thermal	✓	✓			

1.4 Objectives

The main objective of this thesis is to develop a tool for selecting the optimum renewable energy powered desalination system for a given city in the world given renewable energy data and production capacity required. This main objective is divided into a number of tasks. These tasks are as follows:

1. Study each renewable energy system and resources carefully.
2. Develop a mathematical model for each renewable energy system based on power output.
3. Develop a cost model including installation, land, maintenance and operation costs.
4. Study each desalination system carefully including the development of thermodynamics and cost models.
5. Study cost-effective and energy-efficient combinations between renewable energy systems and desalination systems.
6. Develop a computerized selection tool to obtain the optimum renewable powered desalination system.

1.5 Selection Methodology

To come up with the optimum selection of renewable energy powered desalination system the following methodology is followed:

- Based on water capacity needed and feed-water salinity, the energy needed to desalinate the required capacity of water using different desalination systems such as reverse osmosis, multi-effect desalination is evaluated.
- Cost models are used to estimate installation, operation & maintenance and total costs.
- Using renewable energy data, renewable power generation-systems sizes that used to power the desalination systems are evaluated. Renewable energy generation systems include solar-thermal, solar PV and wind turbine.
- Cost models are also used to estimate installation, operation & maintenance and total costs.
- Specific cost per one cubic meter of distillate water is obtained for each renewable-desalination combination using cost of both systems.
- Specific costs for all combinations are compared and the combination that has the lowest specific cost is selected as the optimum renewable powered desalination system.

Figure 13 shows the main objective of this thesis represented as a tool given renewable resources in a specific location with water capacity needed and feed-water salinity and it will provide the user with the optimum renewable energy-powered desalination system.

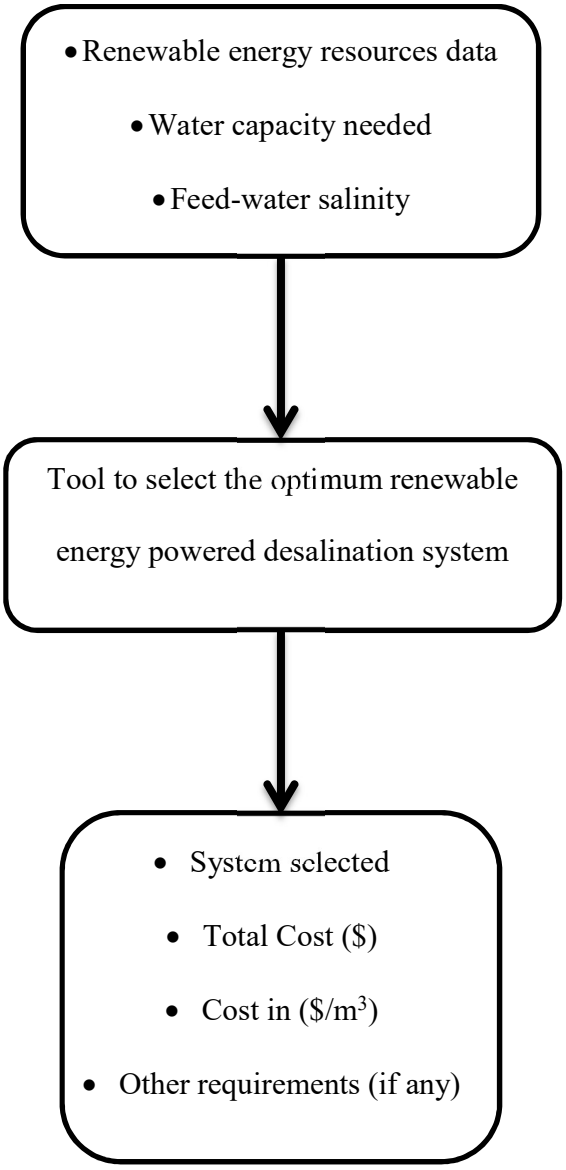

Figure 13: Optimization tool representation.

CHAPTER 2

LITERATURE REVIEW

Research and development of desalination technologies are becoming highly important because of the rapid increase of the need of fresh water. Researchers are continually working on improving the existing technologies and exploring new methods and ideas to desalinate salty water. Main researches' goal is to come up with cost-effective system. Renewable energy powered desalination systems are introduced to overcome the rising oil and fossil-fuels prices.

(Chauhan & Saini, 2014) presented a comprehensive review of integrated renewable energy systems including configuration, models, storage options and others. (Kalogirou, 2005) reviewed industrially-proven desalination and renewable systems. Indirect solar desalination has been comprehensively reviewed by (Ali, et al., 2011). (Gude, et al., 2010) discussed desalination systems and possible utilization of renewable energy. They suggested coupling renewable systems and reusing and recycling of water and energy. (Eltawil, et al., 2009) in their renewable energy powered desalination systems review indicate that the implementation of these systems are slow mainly because of governmental subsides. Evaluation of renewable potential in the Arab regions has been done by (Al-Karaghouli, et al., 2009) with brief

description of desalination and renewable systems. In wind energy powered desalination review, (Ma & Lu, 2011) concluded that these systems are technically mature although system installation is limited. Their observation was that RO is the most desalination technology powered by wind. (Karagiannis & Soldatos, 2008) provided water desalination cost review and they concluded that the cost of water is location dependent.

Desalination is recognized as energy-intensive process because it is consuming large amount of energy and energy, in average, represent 50% of the production cost of water. For distillation processes, energy represents 60% of the production cost; it will be much lower in cogeneration plants where turbine exhaust is the energy source. However, it is representing only 44% in RO mainly because reverse osmosis consumes less energy than distillation technologies including MSF and MED (Al-Karaghouli & Kazmerski, 2013). In general, distillation methods and reverse osmosis are used for seawater while reverse osmosis and eletrodialysis are used for brackish water (Al-Karaghouli, et al., 2009).

(Al-Karaghouli & Kazmerski, 2013) stated that desalination technologies powered by renewable energy is proven technology and economically competitive in remote regions. Technology improvement and/or fossil-fuel prices rising will make these systems economically viable. (Al-Karaghouli, et al., 2009) indicated that solar

powered desalination with capacity less than 10 m^3 per day in remote area, where fuel, grid and technical support are unavailable, is the only technology that is technically and economically competitive to other technologies. (Ghaffoura, et al., 2015) claimed that solar desalination cost exceeds conventional systems cost by more than four times and cannot be reduced to compete the conventional costs by the near future.

Solar and wind energy coupled with desalination systems have been implemented and seems to be promising more than other renewable-desalination combinations (Gude, et al., 2010). The most renewable-desalination combination used are PV-RO (Ghaffoura, et al., 2015), (Kalogirou, 2005) and solar thermal-MED (Kalogirou, 2005). Table 4 and Table 5 show the worldwide breakdown of renewable energy powered desalination capacity based on desalination technology and renewable energy respectively.

Table 4: Worldwide desalination technology driven by renewable energy

(Gude, et al., 2010)

Desalination Technology	Percentage (%)
RO	62
ED	5
MSF	10
MED	10
VC	5
Others	4

Table 5: Worldwide renewable energy powering desalination systems (Gude, et al., 2010)

Renewable Energy	Percentage (%)
PV	43
Solar thermal	27
Wind	20
Hybrid	10

The selection of the appropriate method should go through a careful study of location conditions and local circumstances (Al-Karaghouli, et al., 2009). (Gude, et al., 2010) mentioned several parameters that affect the decision of the selection. These parameters include plant capacity, feed-water salinity, availability of grid, technical support and infrastructure, remoteness and local renewable resources.

(Ettouney, 2004) and (Nafey, et al., 2006) provided tools to design and simulate several desalination systems including different types and configurations. The systems include MSF, MED, MED-TVC, MED-MVC and RO. (Abdul-Fattah, 1986)

compared five different solar desalination systems based on previously set objectives. He concludes that solar PV-RO system is the best. (Rheinländer, et al., 2003) have developed a simulation tool for de-centralized supply of power and water. Power sources are renewable (wind and solar PV) and conventional (Diesel). (Perz & Bergmann, 2007) adapted the simulation tool by adding economical models for techno-economic analysis. A comparison between four different renewable-desalination combinations has been carried by (Koroneos, et al., 2007). The result shows that RO-Wind and MVC-Wind has almost the same specific cost of 1.49 and 1.5 EURO/m^3, respectively. RO-PV is costing 2.77 EURO/m^3 while MVC-PV with the height cost of 3.67 EURO/m^3.

Based on the above literature, it is seen that the comparisons between different desalination technologies and specifically renewable powered desalination technologies were mainly based on different system capacity, energy source system, feed-water salinity and system components. This makes the economical comparison almost impossible. There is an existing gap in having an economical comparison to different renewable powered desalination systems with the same basics such as availability of renewable and water resources. This research is an attempt to provide a tool to fulfill this gap.

2.1 Thermodynamics modeling of power systems

(Zhou, et al., 2010) reviewed solar PV-wind power systems with battery storage with respect to different simulation, optimization and control techniques. (Deshmukh & Deshmukh, 2008) have reviewed and presented modeling of different renewable energy components and their hybridization. Hybrid solar PV-wind-battery optimization procedure is presented in (Habib, et al., 1999). (Groumpos & Papageorgiou, 1987) developed an algorithm for optimal sizing of standalone PV-battery power system. (Yang, et al., 2009) developed genetic algorithm to optimize several parameters of hybrid solar PV-wind-battery system. The parameters are number of PV modules and their slope angle, number of wind turbines and their height and number of batteries.

2.2 Thermodynamics modeling of renewable energy powered desalination systems

Two renewable energy systems (Wind & solar PV) and two desalination systems (RO & MVC) are compared and modeled by (Koroneos, et al., 2007). Authors claim that expensive energy storage is the main limitation of application expansion. (Mohamed & Papadakis, 2004) developed a simplified design of hybrid wind-PV-storage system powering SWRO. They conclude that using pressure exchanger could reduce the production cost by 48%. (Mokheimer, et al., 2013) have modeled and optimized a hybrid wind-solar powered reverse osmosis. (Miranda & Infield, 2003) presented a

reverse osmosis system powered by wind turbine without using a battery. (Ahmad, et al., 2015) have modeled and simulated solar PV-RO system and the model is validated experimentally. A drawn conclusion is that single and double axis tracking of PV would increase the water production by 43% and 62%, respectively. Designing of solar thermal reverse osmosis is presented by (Peñate & García-Rodríguez, 2012). (Nafey & Sharaf, 2010) presented energy, exergy and cost analysis of solar thermal reverse osmosis. The analysis of solar thermal energy includes flat plate collector, parabolic trough and compound parabolic concentrator.

CHAPTER 3

MEMBRANE DESALINATION SYSTEMS

To reach to the research main objective, several thermodynamics and economics models for desalination and renewable systems have to be studied and validated with literature. Two combinations are presented here which are RO-Wind and RO-PV. Both of them following the same methodology except that in Wind-RO monthly average daily wind speed is used while in RO-PV a representative day in each month is selected and full-day simulation is used. Therefore, only the methodology of RO-Wind is presented.

In order to come up with the appropriate design of Wind-RO, the following methodology is applied. The presented methodology uses water storage to ensure water availability instead of energy storage. This selection makes the system more reliable, more economical, feasible especially for large capacity, more environmentally friendly and it is in line with our primary goal of water production. The methodology is as the following:

- Based on water capacity needed ($M_{n,avg}$) and feed-water salinity, the size needed to desalinate the required capacity of water using reverse osmosis

desalination system is evaluated. The size of RO system is mainly determined by number of pressure vessels ($N_{Pressurevessels}$).

- Once the size of the RO system is decided, the power required is evaluated then the number of wind turbines ($N_{Turbines}$) is determined using yearly average wind speed.
- Power produced by wind farm in each month is evaluated ($P_{wind,i}$, i=1,12) based on actual weather data.
- Monthly and Monthly average water production is evaluated ($M_{d,i}$, i=1,12 & $M_{d,avg}$) based on monthly power production.
- In some months, all energy produced is utilized to desalinate water. In others, energy produced is more than the maximum power required by the desalination system so some of the energy is excess. Excess of Energy (EE) is evaluated.
- If average water production is less than average water demand and there is no excess of energy this means the power system is not enough to produce the required water capacity so we need to size up the power system by one additional turbine. If there is energy excess, we increase the size of the RO system by adding one pressure vessel.
- Finally, the storage tank status is evaluated at the end of each month ($Tank_i$, i=1,12) to insure availability of water. Size of storage tank is determined by the maximum water volume available in storage tank at the end of each month and the minimum storage size is determined by water demand for 30 days.

- Total and specific cost of power, desalination and storage systems are evaluated.

The above explained methodology for RO-Wind is depicted in Figure 14.

As previously mentioned, the methodology followed in RO-PV is very similar to RO-Wind except in having full-day operation evaluation for an average day in each month.

It is important to recall that we use water storage instead of energy storage. For this purpose, the status of the tank is monitored for the first twelve months to guarantee water supply by the system in all months. Size of the tank is determined by the maximum water storage volume required and the minimum storage tank size is determined by water demand for one month. Water production is not the same in all months. It is a function of renewable resources available and renewable power system size. So, water production in some months will be more than the needed to balance the months with lower renewable resources. Therefore, status of water storage tank is strongly dependent of the starting month.

To demonstrate the presented methodology, cases of both RO-Wind and RO-PV are analyzed. The fixed parameters for which these cases are analyzed are summarized in Table 6. The analysis is done for Dhahran, Saudi Arabia. Renewable resources for Dhahran including monthly average daily solar insolation ($kWh/m^2/day$), monthly average wind speed and monthly average mean temperature are shown in Table 7.

Table 6: Fixed Design Parameters of RO-Wind and RO-PV cases

Quantity (unit)	Value
Daily water demand (m^3)	1,000
Feed water salt concentration (PPM)	45,000
Feed water Temperature (°C)	25
Recovery Ratio (%)	30
Membrane Area (m^2)	35.4
Number of elements in each pressure vessel (-)	7

Table 7: Monthly average weather data for Dhahran, Saudi Arabia (Habib, et al., 1999)

Month	Insolation ($kWh/m^2/day$)	Wind speed (m/s)	Mean temperature (°C)
January	3.348	5.95	14.4
February	4.377	5.70	16.8
March	5.181	5.50	20.9
April	6.257	4.80	25.5
May	6.970	5.40	31.6
June	7.870	6.60	35.8
July	7.344	4.90	37.3
August	6.965	4.70	36.6
September	6.343	4.30	33.2
October	5.249	4.90	30.3
November	4.091	6.05	23.6
December	3.336	6.00	19.0

To apply the proposed methodology, thermodynamics and economical modeling of solar photovoltaic, wind and reverse osmosis are developed. These models are presented in the following sections. Each model is validated against previous work.

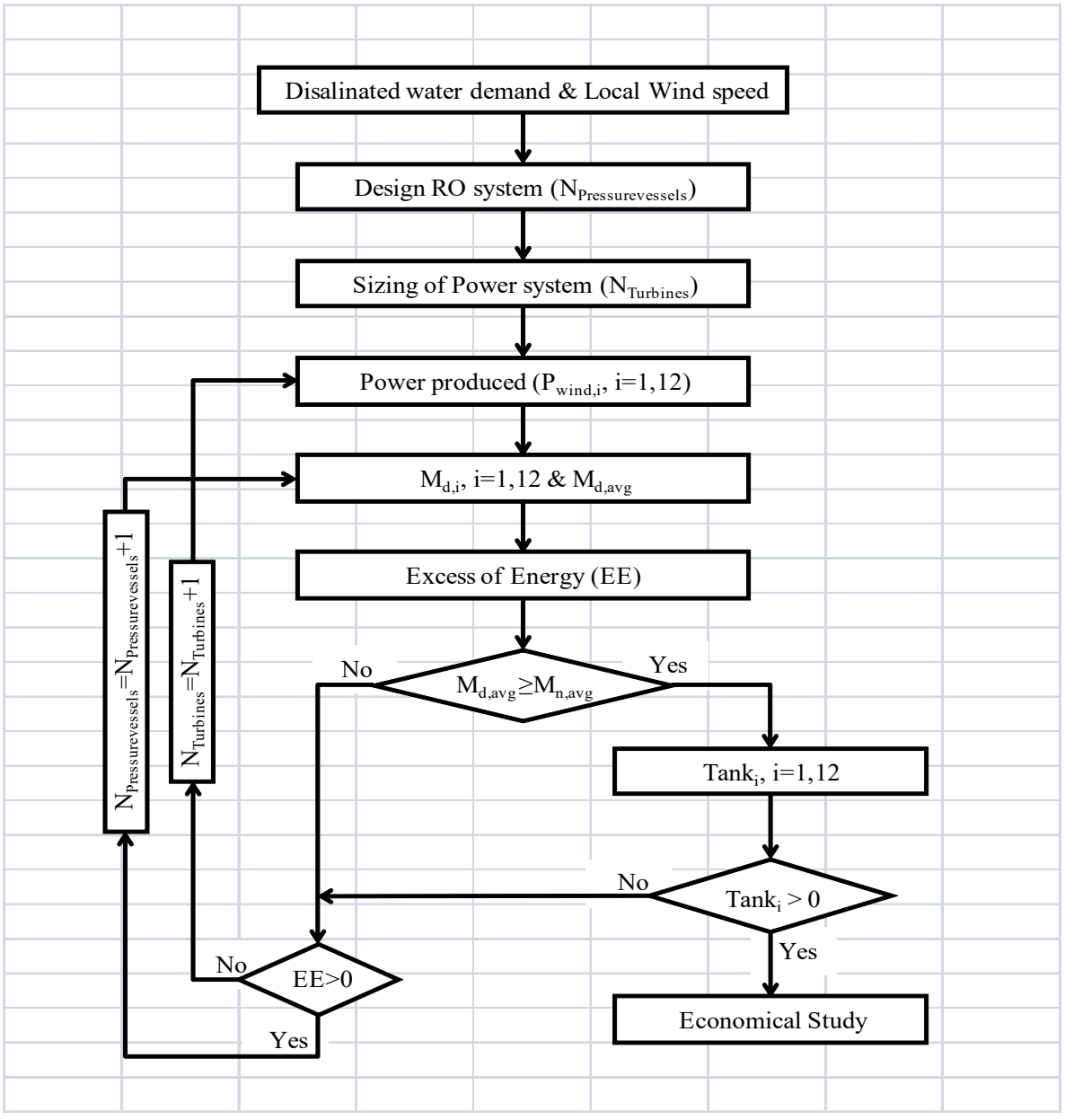

Figure 14: Flowchart of the presented methodology for RO-Wind

3.1 Photovoltaic (PV) Power Modeling

The modeling of a PV array included the solar radiation modeling and PV power generation modeling. The solar radiation modeling estimates the radiation incident on a tilted surface. The PV generation model estimates the PV array output power based on the incident solar radiation, weather conditions and PV panel specification.

In the present analysis, the incident solar radiation is evaluated for each hour in an average day in each month.

Table 8 shows average days in each month and their number of the day in the year, n. Radiation on horizontal surface is obtained using the relationship between hourly, I, and daily, H, total radiation on horizontal surface expressed as equations (1) and (2):

$$r_t = \frac{I}{H} \tag{1}$$

$$r_t = \frac{\pi}{24}(a + b\ \cos\omega)\left[\frac{\cos\omega - \cos\omega_s}{\sin\omega_s - \frac{\pi\omega_s}{180}\cos\omega_s}\right] \tag{2}$$

$$a = 0.409 + 0.5016\sin(\omega_s - 60)$$

$$b = 0.6609 - 0.4767\sin(\omega_s - 60)$$

where ω is the hour angle in degrees and ω_s is the sunset hour angle which could be found by equation (3):

$$\cos \omega_s = -\tan \phi \tan \delta \quad \textbf{(3)}$$

where ϕ is the latitude and δ is the declination angle of the sun and could be approximated by Cooper's equation "1969" (4):

$$\delta = 23.45\, sin\left(360\left(\frac{284+n}{365}\right)\right) \quad \textbf{(4)}$$

Table 8: Average days in each month and number of the day in the year (Duffie & Beckman, 2006)

Month	Date	n
January	17	17
February	16	47
March	16	75
April	15	105
May	15	135
June	11	162
July	17	198
August	16	228

September	15	258
October	15	288
November	14	318
December	10	344

Total radiation on tilted surface based on isotropic diffuse model is composed of three main components: beam, diffuse and reflected and it is evaluated by equation (5):

$$I_T = I_b R_b + I_d \left(\frac{1+\cos\beta}{2}\right) + I\,\rho_g \left(\frac{1-\cos\beta}{2}\right) \quad \textbf{(5)}$$

In order to evaluate I_b and I_d, Erbs et al. suggested correlation (6):

$$\frac{I_d}{I} = \begin{cases} 1.0 - 0.09\,k_T & for\ k_T \le 0.22 \\ 0.9511 - 0.1604k_T + 4.388{k_T}^2 - 16.638{k_T}^3 & \\ \quad +12.336{k_T}^4 & for\ 0.22 < k_T \le 0.8 \\ 0.165 & for\ k_T \le 0.8 \end{cases} \quad \textbf{(6)}$$

where k_T is hourly clearness index and it is defined as $k_T = I/I_o$

I_o is the extraterrestrial radiation on a horizontal surface for an hour period of time bounded by hour angles $\omega_2$and ω_1 where $\omega_2$is larger. Extraterrestrial radiation could be found by equation (7):

$$I_o = \frac{12 \times 3600}{\pi} G_{sc} \times \left(1 + 0.033 \cos\left(\frac{360\, n}{365}\right)\right) \times \left[\cos\phi \cos\delta \left(\sin\omega_2 - \sin\omega_1\right) + \left(\frac{\pi(\omega_2 - \omega_1)}{180}\right) \sin\phi \sin\delta\right] \quad \textbf{(7)}$$

G_{sc} is solar constant and it is equal to 1367 W/m^2 or 4.92 MJ/m^2.hr.

Now, diffuse and beam radiation are evaluated by equations (8):

$$I_d = \left(\frac{I_d}{I}\right) \times I \qquad \& \qquad I_b = \left(1 - \frac{I_d}{I}\right) I \quad \textbf{(8)}$$

Ratio of beam radiation on tilted surface to that on horizontal surface (R_b) is defined for the northern hemisphere as equation (9):

$$R_b = \frac{\cos(\phi - \beta)\cos\delta\cos\omega + \sin(\phi - \beta)\sin\delta}{\cos\phi\cos\delta\cos\omega + \sin\phi\sin\delta} \quad \textbf{(9)}$$

where β is the slope of tilted surface.

ρ_g is ground reflectance and it is taken as 0.2 for Dhahran, Saudi Arabia (Ahmad, et al., 2015).

This is a complete modeling to find total solar radiation of a tilted surface. PV power generation can be obtained by the model presented in (Ahmad, et al., 2015). PV power

generation is strong function of solar radiation and cell temperature. Cell temperature (T_c) can be found by equation (10) :

$$T_c = T_a + I_T \left(1 - \frac{\eta_c}{\tau\alpha}\right)\left(\frac{\tau\alpha}{U_L}\right) \quad \textbf{(10)}$$

where T_a is ambient temperature, $\eta_c$is electrical conversion efficiency, τ is solar transmittance of PV module, α is solar absorption of the module and $U_L$is overall loss coefficient. The quantity $\tau\alpha/U_L$ could be estimated by equation (11):

$$\frac{\tau\alpha}{U_L} = \frac{T_{C,NOCT} - T_{a,NOCT}}{I_{T,NOCT}} \quad \textbf{(11)}$$

$T_{C,NOCT}$ is Normal Operating Cell Temperature (NOCT) which is defined as the cell temperature at no load operation ($\eta_c = 0$), an incident radiation($I_{T,NOCT}$) of 800 W/m^2, an ambient temperature ($T_{a,NOCT}$) of 20 C with an average wind speed of 1 m/s.

Cell efficiency $\eta_c$is assumed to be equal to maximum power point efficiency (η_{mp}) and it is equal to (12):

$$\eta_c = \eta_{mp} = \eta_{mp,std}\left[1 + \alpha_p(T_c - T_{c,std})\right] \quad \textbf{(12)}$$

where $\eta_{mp,std}$ is the maximum efficiency under standard reference conditions which are radiation ($I_{T,stc}$) of 1000W/m^2, cell temperature ($T_{c,std}$) of 25 C, air mass ratio of 1.5 and zero wind speed. α_p is temperature degradation coefficient.

PV output power could be calculated by equation (13):

$$P_{mp} = P_{mp,std}\left(\frac{I_T}{I_{T,st}}\right)\left[1 + \alpha_p(T_c - T_{c,std})\right] \quad \textbf{(13)}$$

where $P_{mp,std}$ is cell maximum power at standard reference conditions.

The presented PV power generation model was implemented in Engineering Equation Solver (EES) software package. The developed model is validated against the results presented in (Ahmad, et al., 2015).

3.2 Wind Power Modeling

Wind power is one of the most important renewable power systems. In this section, a mathematical model of the wind turbine is presented. The dominant parameter that affects the wind turbine output is the wind speed. When evaluating the power output from wind turbine, wind speed has to be calculated at the turbine elevation. Equation (14) is used where υ and υ_o are wind speeds at hub height z and reference height z_o, respectively. α is the ground surface friction coefficient and typically taken as (1/7) (Mokheimer, et al., 2013).

$$\frac{v}{v_o} = \left(\frac{z}{z_o}\right)^{\alpha} \tag{14}$$

Wind turbine power output is usually evaluated using its own characteristic curve. For programming purposes, curve fitting is used for the evaluation. To guarantee best fitting, several polynomials as shown in equation (15) are used.

$$P_W(v) = \begin{cases} 0 \quad , & v < v_c \\ a_1 v^n \ldots b_1 v^2 + c_1 v + d_1 \, , & v_c \le v < v_1 \\ a_2 v^n \ldots b_2 v^2 + c_2 v + d_2 \, , & v_1 \le v < v_2 \\ a_3 v^n \ldots b_3 v^2 + c_3 v + d_3 \, , & v_2 \le v < v_3 \\ 0 \quad , & v > v_f \end{cases} \tag{15}$$

where υ_c and υ_f are the cut-in and cut-off wind speed of the wind turbine.

Presented wind turbine model is validated with (Elhadidy & Shaahid, 2005). In their work, they have three different wind farms, each of 6 MW capacity. The three farm are: forty wind turbines of 150 kW, twenty-four wind turbines of 250 kW and ten wind turbines of 600 kW. Table 9 shows the monthly average daily energy generated

by forty wind turbines, each of 150 kW. The model uses the monthly average wind speed for the year 1992 and turbine hub height of 50 meters. Figure 15 shows the difference between the presented model and (Elhadidy & Shaahid, 2005) model. Similar procedure is applied to twenty-four wind turbines of 250 kW and the results are shown in Table 10 and Figure 16. Results of ten wind turbines of 600 kW are shown in Table 11 and Figure 17.

In general, the two models show good agreement except for June and July. Over estimation of wind speed at these months could be the reason because wind speeds at these months are the maximum.

Table 9: Monthly average daily energy (kWh) generated from forty turbines of 150 kW

Month	Developed Model	(Elhadidy & Shaahid, 2005)	%
January	89899	75265	19.44%
February	85628	71307	20.08%
March	59210	57624	2.75%
April	56462	53840	4.87%
May	65539	62074	5.58%
June	134547	93535	43.85%
July	111289	90200	23.38%
August	51666	53774	3.92%
September	43613	46199	5.60%
October	41615	44800	7.11%
November	53959	56224	4.03%
December	81312	73784	10.20%
AVG	72834	64877	12.26%

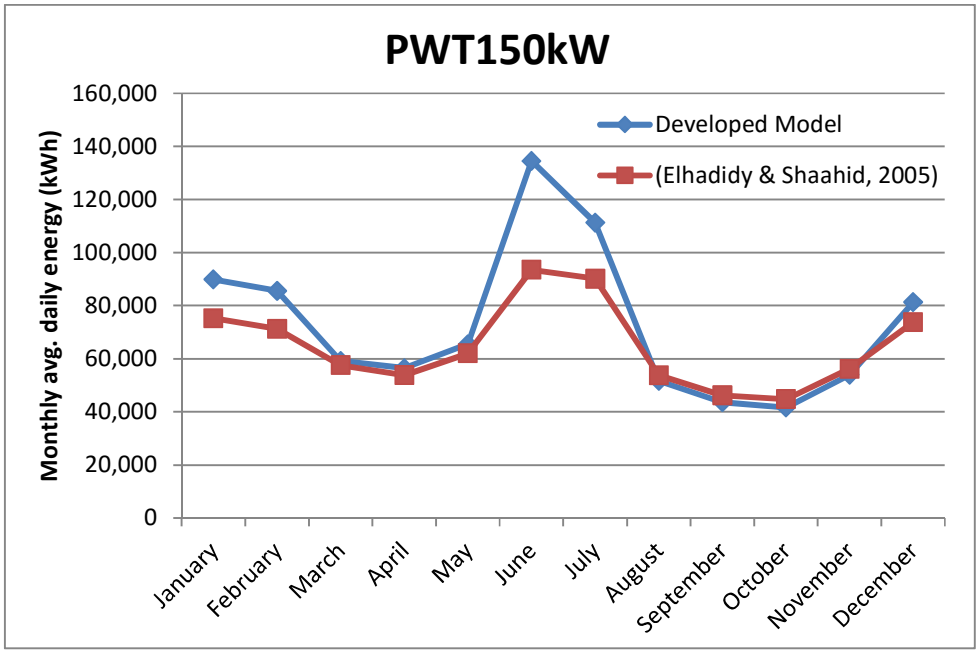

Figure 15: Comparison between developed model and (Elhadidy & Shaahid, 2005) model for forty turbines of 150 kW

Table 10: Monthly average daily energy (kWh) generated from twenty four turbines of 250 kW

Month	Developed Model	(Elhadidy & Shaahid, 2005)	%
January	58314	54045	7.90%
February	55612	51364	8.27%
March	38315	41014	6.58%
April	36138	38729	6.69%
May	42911	44869	4.36%
June	91337	69669	31.10%
July	77837	66556	16.95%
August	32041	38218	16.16%
September	24883	33125	24.88%
October	23302	31433	25.87%
November	34047	40414	15.75%
December	52955	52376	1.11%
AVG	47270	46807	0.99%

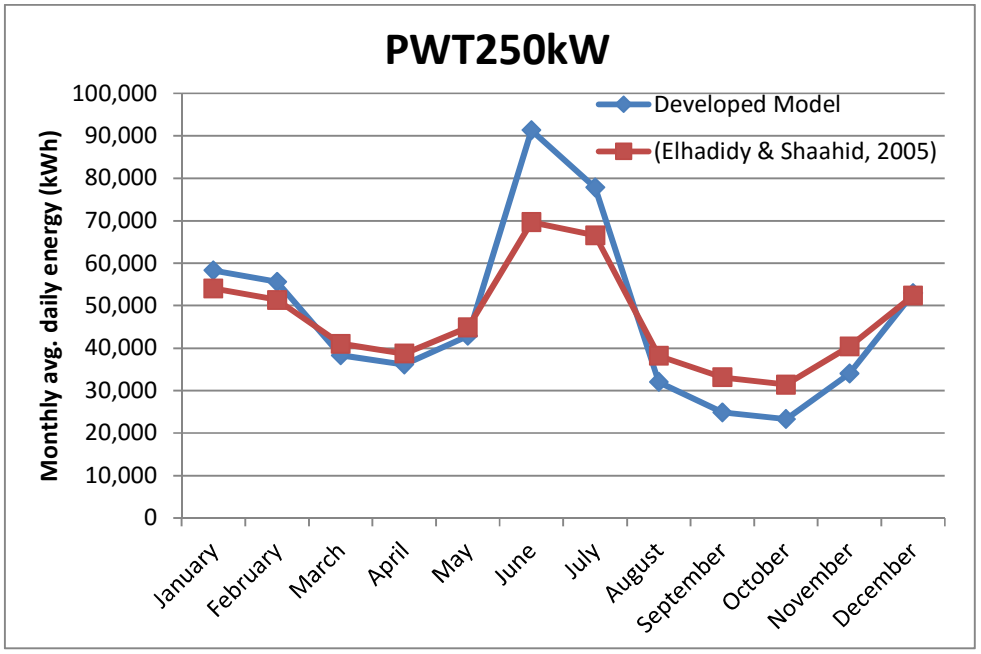

Figure 16: Comparison between developed model and (Elhadidy & Shaahid, 2005) model for forty turbines of 250 kW

Table 11: Monthly average daily energy (kWh) generated from ten turbines of 600 kW

Month	Developed Model	(Elhadidy & Shaahid, 2005)	%
January	53022	51273	3.41%
February	50482	48292	4.53%
March	34219	37680	9.19%
April	32135	35062	8.35%
May	38574	41802	7.72%
June	86308	67457	27.95%
July	71966	64944	10.81%
August	28161	34725	18.90%
September	21012	29648	29.13%
October	19395	27532	29.55%
November	30115	37189	19.02%
December	47992	49513	3.07%
AVG	42744	43751	2.30%

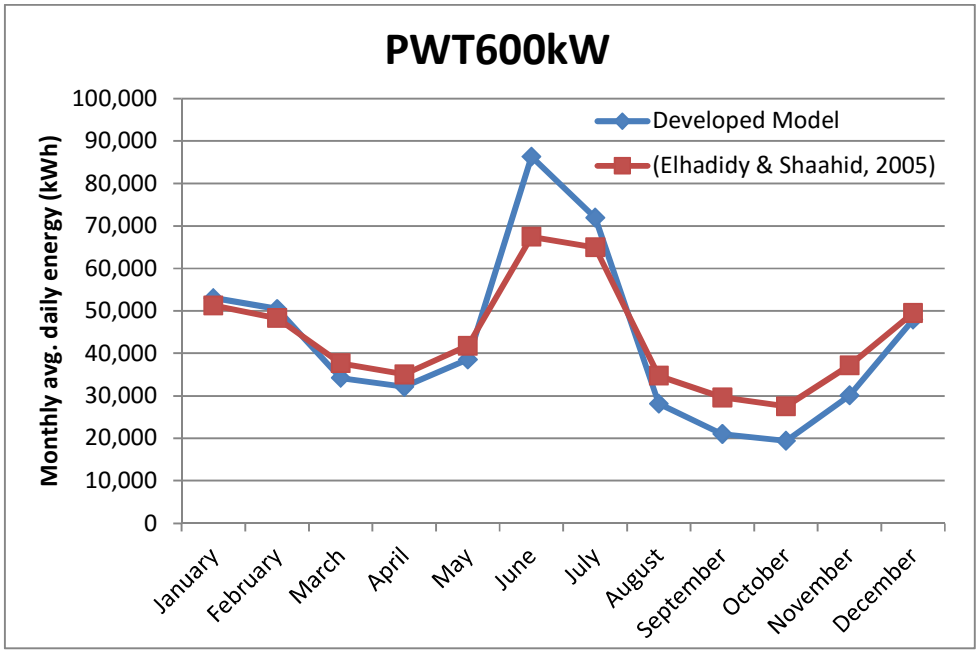

Figure 17: Comparison between developed model and (Elhadidy & Shaahid, 2005) model for ten turbines of 600 kW

3.3 Reverse Osmosis Modeling

The mathematical thermodynamics model of RO system is developed as presented in (El-Dessouky & Ettouney, 2002).

Recovery Ratio is the ratio of distillate mass flow rate to feed mass flow rate:

$$\text{Recovery Ratio} = \frac{\mathrm{M}_{\mathrm{distillate}}}{\mathrm{M}_{\mathrm{feed}}} \quad \textbf{(16)}$$

Salt rejection percentage:

$$\text{Salt Rejection} = \frac{X_{\mathrm{feed}} - X_{\mathrm{distillate}}}{X_{\mathrm{feed}}} \quad \textbf{(17)}$$

where X is Salt concentration

Mass conservation equation:

$$\mathrm{M}_{\mathrm{feed}} = \mathrm{M}_{\mathrm{distillate}} + \mathrm{M}_{\mathrm{brine}} \quad \textbf{(18)}$$

Salt mass conservation equation:

$$\mathrm{M}_{\mathrm{feed}} \times X_{\mathrm{feed}} = \mathrm{M}_{\mathrm{distillate}} \times X_{\mathrm{distillate}} + \mathrm{M}_{\mathrm{brine}} \times X_{\mathrm{brine}} \quad \textbf{(19)}$$

Average salt concentration $\overline{X}$ is equal to:

$$\overline{X} = \frac{\mathrm{M}_{\mathrm{feed}} \times X_{\mathrm{feed}} + \mathrm{M}_{\mathrm{brine}} \times X_{\mathrm{brine}}}{\mathrm{M}_{\mathrm{feed}} + \mathrm{M}_{\mathrm{brine}}} \quad \textbf{(20)}$$

Distillate water salt concentration could be found by equation (21):

$$X_{\text{distillate}} = \frac{\text{M}_{\text{salt}}}{\text{M}_{\text{distillate}}} \tag{21}$$

where M_{salt} for each membrane is evaluated by equation (22):

$$\text{M}_{\text{salt}} = \left(\overline{X} - X_{\text{distillate}}\right) k_S \, A \tag{22}$$

Temperature correction factor TCF equation:

$$TCF = \exp\left[2700 \times \left(\frac{1}{T + 273} + \frac{1}{298}\right)\right] \tag{23}$$

where T is the feed water temperature.

Membrane water permeability k_w:

$$k_w = 6.84 \times 10^{-8} \times \frac{18.6865 - (0.177 \times X_{\text{brine}})}{T + 273} \tag{24}$$

Membrane salt permeability k_S:

$$k_S = FF \times TCF \times 4.72 \times 10^{-7} \times \left[0.06201 - \left(5.31 \times 10^{-5} \times (T + 273)\right)\right] \tag{25}$$

where FF is the fouling factor and it is equal to one for new membrane.

An approximation for osmotic pressure is obtained by assuming 1000 ppm of Total Dissolved Solids (TDS) equals to 75.84 kPa of osmotic pressure. So osmotic pressure is equal to:

$$\Pi = 75.84 \times X \qquad \text{for feed, distillate and brine} \tag{26}$$

Average osmotic pressure:

$$\Pi_{avg} = 0.5 \times \left(\Pi_{feed} + \Pi_{brine}\right) \tag{27}$$

Net osmotic pressure:

$$\Delta\Pi = \Pi_{avg} - \Pi_{distillate} \tag{28}$$

Net pressure difference:

$$\Delta P = \left(\frac{\mathrm{M}_{\mathrm{distillate}}}{TCF \times FF \times A \times n_e \times n_v \times k_W}\right) + \Delta\Pi \tag{29}$$

where A is element area; n_v is number of pressure vessels; n_e is number of elements in each pressure vessel.

Power required for RO driving pump in (kW) is evaluated by equation (30):

$$HP = \left(\frac{\mathrm{M}_{\mathrm{distillate}} \times \Delta P}{\eta_{pump}}\right) \tag{30}$$

Specific power consumption:

$$SPC = \frac{HP}{\mathrm{M}_{distillate}} \quad \textbf{(31)}$$

Using Engineering Equation solver (EES) packages, RO mathematical model (equations 16-31) is implemented. Results are validated against the results presented in (Nafey & Sharaf, 2010).

Table 12 shows the results obtained using the developed model and results obtained in different models used in (Nafey & Sharaf, 2010).

Table 12: Validation of RO mathematical model

Parameter	Presented Model	Model used in (Nafey & Sharaf, 2010)	VDS	ROSA6.1	Unit
			As presented in (Nafey & Sharaf, 2010)		
SPC	7.921	7.68	7.76	7.76	kWh/m^3
HP	1155	1131	1130	1131.42	kW
M_f	486	485.9	486	458.9	M^3/h
M_b	340.2	340.1	340.23	340.15	M^3/h
X_b	64,179	64,180	66,670	62,005	PPM
X_d	250	250	200	283.83	PPM
SR	0.9944	0.9944	0.9927	-	-
ΔP	6843	6850	6700	6670	kPa

Cost evaluation for reverse osmosis plant is obtained by the model presented in (Nafey & Sharaf, 2010). Total cost is mainly based on two components, Capital and Operation & Maintenance costs. Total capital cost (TCC) is evaluated as equation (32):

$$TCC = DCC + ICC \quad \textbf{(32)}$$

where direct capital cost (DCC) is composed of:

$$DCC = CC_{equip} + CC_{site} \quad \textbf{(33)}$$

Equipment capital cost($\mathrm{CC_{equip}}$) is mainly divided into:

$$CC_{equip} = CC_{swip} + CC_{hpp} + CC_e \quad \textbf{(34)}$$

Seawater intake and pretreatment (CC_{swip}) and high pressure pump (CC_{hpp}) capital costs are evaluated as presented in (Malek, et al., 1996):

$$CC_{swip} = 996 \times {M_{feed}}^{0.8} \quad \textbf{(35)}$$

$$CC_{hpp} = 393{,}000 + 10{,}710 \times \Delta P_f \quad \text{where } \Delta P_f \text{ is feed pressure} \quad \textbf{(36)}$$

Elements capital cost (CC_e) is evaluated by equation (37):

$$CC_e = P_P \times n_e \times n_v + PV_P \times n_v \quad \textbf{(37)}$$

where P_P and PV_P are unit costs of membrane elements and pressure vessels, respectively.

Site capital cost (CC_{site}) is estimated to be 10% of equipment capital cost (CC_{equip}). Also, Indirect capital cost (ICC) is estimated as 27% of the direct capital cost (DCC). Total capital cost (TCC) is the summation of direct and indirect capital costs.

Annual capital cost (ACC) is evaluated by equation (38):

$$ACC = TCC \times A_f \tag{38}$$

where A_f is called the amortization factor and it is found by equation (39):

$$A_f = \frac{i(1+i)^{LT_P}}{(1+i)^{LT_P} - 1} \tag{39}$$

where i is the interest rate and it is equal to 5%. LT_P is the life time of the project and it is equal to 20 years.

Total operational cost (OC_{Total}) is composed of power (OC_{Power}), labor (OC_{Labor}), chemicals (OC_{chm}), insurance (OC_{insur}), and membrane (OC_{memb}) operational costs. Each of them is evaluated as equations (40)-(44):

$$OC_{Power} = LF \times 0.06 \times SPC \times M_{distillate} \tag{40}$$

$$OC_{Labor} = LF \times 0.01 \times M_{distillate} \tag{41}$$

$$OC_{chm} = LF \times 0.04 \times M_{distillate} \tag{42}$$

$$OC_{insur} = 0.005 \times TCC \times M_{distillate} \tag{43}$$

$$OC_{memb} = P_P \times n_e \times \frac{n_v}{LT_m} \quad \textbf{(44)}$$

where LF is the load factor of the plant and it is equal to 0.9, LT_m is the life time of the membrane and it is equal to 5 years. Hourly cost of the RO plant ($/h) is equal to:

$$Z_{RO} = \frac{(ACC + OC_{Total})}{8760} \quad \textbf{(45)}$$

Evaluating RO specific cost of water ($/m^3) can be done now by dividing hourly cost by hourly water production:

$$C_{RO} = \frac{Z_{RO}}{M_{distillate}} \quad \textbf{(46)}$$

CHAPTER 4

THERMAL DESALINATION SYSTEMS

To reach the main research objective, thermodynamics and economics models of concentrated solar power collector and multi-stage desalination have been studied and validated.

4.1 Concentrated Solar Power (CSP)

The mathematical thermodynamics model of Parabolic trough system presented by the National Renewable Energy Laboratory (NREL) in (Forristall, 2003) is used and utilized.

Parabolic troughs where selected over the other CSP technologies because of its higher performance and ability to provide high temperatures. Parabolic trough collectors (PTC) can be operated with one or two axis solar tracking to maximize solar energy absorption. Two axis is exactly following the sun at zero angle. However, it is more difficult to operate and it is not cost-effective. Several one-axis configurations do exist. They are defined based on the axis of rotation. (Gholinejad, et al., 2016) suggest polar axis where the angle between the sun and the collector is equal to the angle of the day (δ). Other configurations include horizontal and vertical rotation axis. The parabolic trough collector used in this analysis is LS-2. The geometrical characteristics of LS-2 are in Table 13.

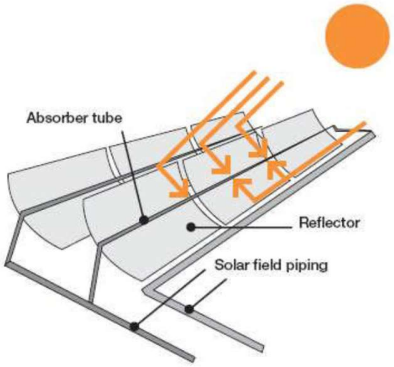

Figure 18: Parabolic trough concentrator

Table 13: Geometric parameters of the solar collector LS-2 (Forristall, 2003)

Parameter	Value
inside diameter of absorber pipe [m]	0.066
outside diameter of absorber pipe [m]	0.070
inside diameter of glass envelope [m]	0.109
Outside diameter of glass envelope [m]	0.115
Aperture's width [m]	4.8235

Cost of solar field collectors and solar pump are obtained using the correlations given by (Sharaf, et al., 2011).

$$\mathrm{DCC_{SolarField}} = 150\mathrm{x}(\mathrm{A}_{col})^{0.95} \quad \textbf{(47)}$$

ICC (Indirect Capital Cost) is considered as 20% of DCC (Direct Capital Cost) and O&M cost is 15% of the Total Capital Cost (TCC)

$$\mathrm{DCC_{Pump}} = 3500\mathrm{x}(\mathrm{W}_{P})^{0.47} \quad \textbf{(48)}$$

ICC is 20% of DCC and O&M cost is 25% of the TCC.

Total Capital Cost (TCC) and O&M Cost are converted to Annual Capital Cost (ACC) by multiplication by A_f (Amortization factor). Amortization factor is evaluated at plant life-time of 20 years and annual interest of 5%.

Annual Electrical Cost (AEC) in ($/year) is evaluated as:

$$\mathrm{AEC} = \mathrm{SEC} \times \mathrm{SPC} \times \mathrm{LF} \times \mathrm{M}_{Distillate} \times 365 \quad \textbf{(49)}$$

Specific Electricity Cost (SEC) is equal to 0.06$/kWh and pump's specific power consumption is in (kWh/m^3), LF is Load Factor and $\mathrm{M}_{Distillate}$ is daily water production in (m^3).

Hourly cost of the solar system ($/h) is equal to:

$$Z_{Solar} = \frac{ACC + AEC}{8760} \quad \textbf{(50)}$$

Evaluating solar thermal specific cost of water ($/m^3) can be done now by dividing hourly cost by hourly water production:

$$C_{Solar} = \frac{Z_{Solar}}{M_{distillate}} \quad \textbf{(51)}$$

4.2 Multi-Effect desalination (MED)

Several MED configurations are presented in literature including forward feed, backward, parallel and parallel/cross. The main difference is the direction of the feed and brine flows.

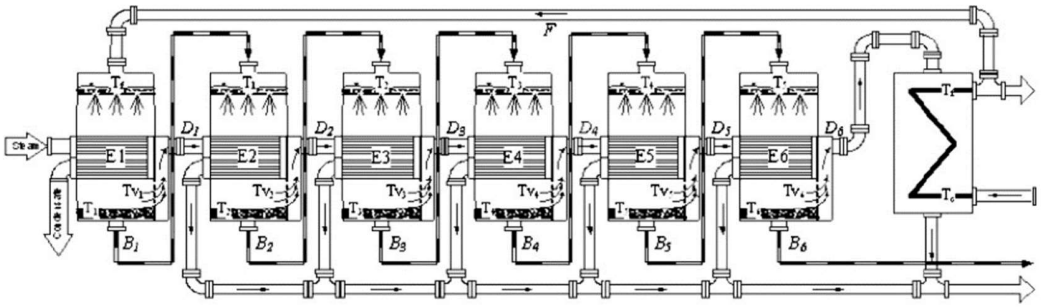

Figure 19: Forward Feed MED Configuration (Sharaf, et al., 2011)

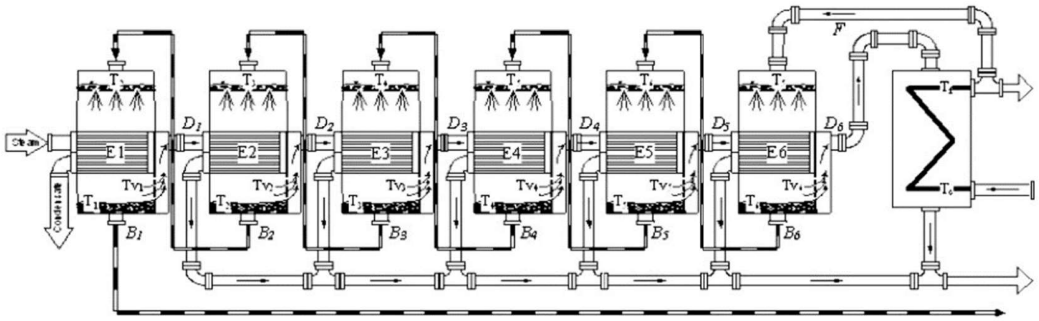

Figure 20: Backward Feed MED Configuration (Sharaf, et al., 2011)

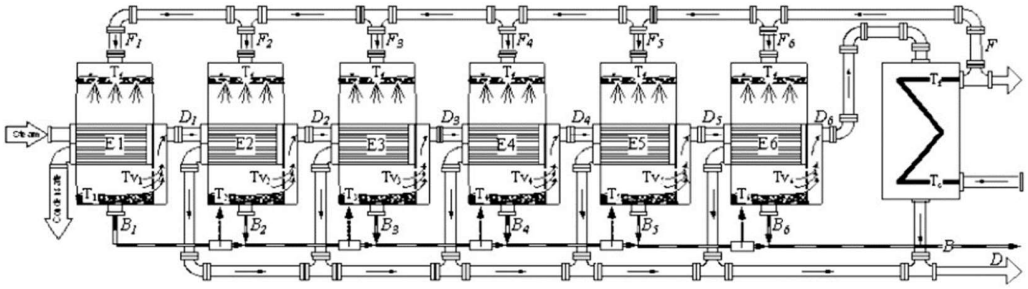

Figure 21: Parallel Feed MED Configuration (Sharaf, et al., 2011)

(Sharaf, et al., 2011) concluded that parallel configuration is the most applicable out of four studied configurations because of its higher gain ratio, specific water cost and areas. The four configurations shown in Figure 19-Figure 21 are forward, backward,

parallel and forward with feed heaters. However, (El-Dessouky, et al., 2000) compared parallel and parallel/cross and they concluded that parallel/cross is more effective than parallel configuration. The main difference between the two configurations is that in parallel/cross the brine of one effect is send to the next effect where flashing is taking place in addition to the vaporization. Both configurations are shown in Figure 22 and Figure 23.

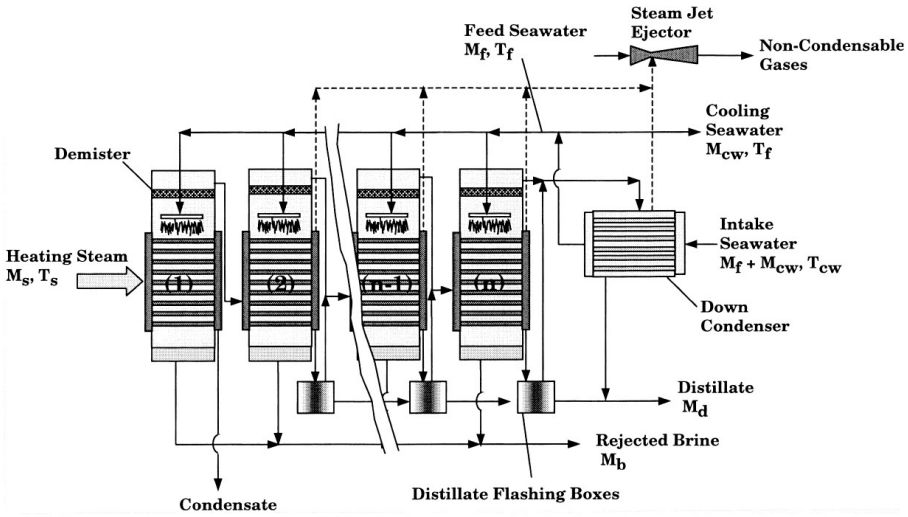

Figure 22: Parallel Feed MED Configuration (El-Dessouky, et al., 2000)

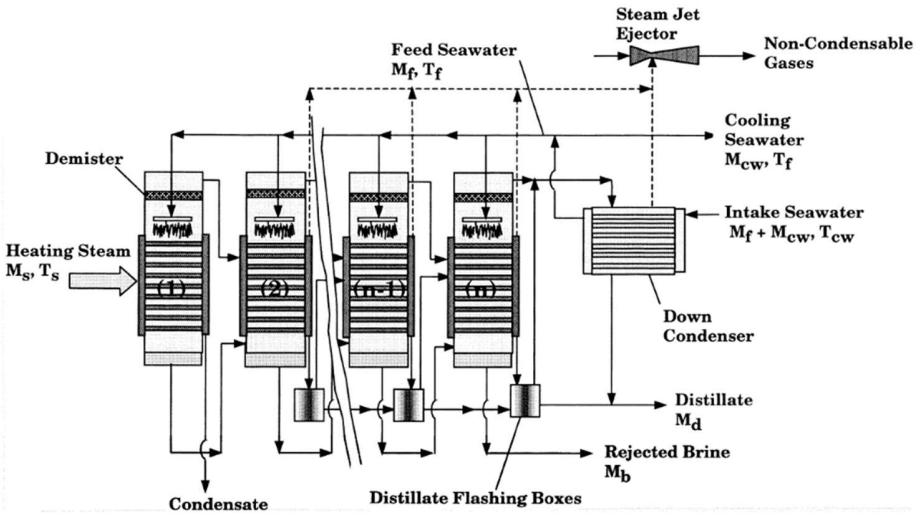

Figure 23: Parallel/cross Feed MED Configuration (El-Dessouky, et al., 2000)

The detailed mathematical thermodynamics model of MED parallel/cross system is developed as presented in (El-Dessouky & Ettouney, 2002) and (El-Dessouky, et al., 2000). Water, salt and energy equations are written for each effect.

First Effect:

Mass Balance:

$$B_1 = F_I - D_1 \quad \textbf{(52)}$$

Salt Balance:

$$x_1 B_1 = F_1 x_f \quad \textbf{(53)}$$

Heat gain by the feed water in the first effect:

$$Q_1 = D_1 h_1 + F_1 C_P (T_1 - T_f) \quad \textbf{(54)}$$

Heat-in in the first effect by external source:

$$Q_1 = \dot{m}_s \lambda_s \quad \textbf{(55)}$$

Energy Equation to obtain heat transfer area:

$$Q_1 = U_{L1} A_e \Delta T_1 \quad \textbf{(56)}$$

Effects 2 to N

$$F_i + B_{i-1} = D_i + B_i \quad \textbf{(57)}$$

Salt balance

$$x_i B_i = x_f F_i + x_{i-1} B_{i-1} \quad \textbf{(58)}$$

$$Q_i = F_i C_p (T_i - T_f) + D_i \lambda_i \quad \textbf{(59)}$$

$$Q_i = (D_{i-1} + d_{i-1} + d'_{i-1}) \lambda_{i-1} \quad \textbf{(60)}$$

where d'_i is the amount of vapor formed by brine flashing and it is evaluated by:

$$d'_i = (B_{i-1}) C_P (T_{i-1} - T'_i) / \lambda_{i-1} \quad \textbf{(61)}$$

where T_i' is the temperature of the cooled down brine and it is equal to:

$$T_i' = \mathrm{T_i} + \mathrm{NEA}_i \tag{62}$$

Heat transfer area can be evaluated by:

$$\mathrm{Q_i} = \mathrm{U_{Li}} \mathrm{A_e} \Delta \mathrm{T_i} \tag{63}$$

where temperature difference is equal to:

$$\Delta \mathrm{T_i} = \mathrm{T_{i-1}} - \mathrm{T_i} \tag{64}$$

Amount of vapor flashed in the flash box:

$$\mathrm{d_i} = \mathrm{D_{i-1}} \mathrm{C}_p \frac{\left(\mathrm{T_{C,i-1}} - \mathrm{T}_i''\right)}{\lambda_i'} \tag{65}$$

where $\mathrm{T_{C,i}}$ and T_i'' are defined as follows:

$$T_{c,i} = \mathrm{T_i} - \mathrm{BPE}_i \tag{66}$$

$$T_i'' = T_{v,i} + NEA_i \tag{67}$$

Condenser:

Heat transfer between the two streams are equal to:

$$\mathrm{Q_c} = (\mathrm{D_N} + \mathrm{d_N} + d'_N)\lambda_\mathrm{N} \quad \textbf{(68)}$$

$$\mathrm{Q_c} = (\mathrm{M_{cw}} + \mathrm{F})\mathrm{C_p}(\mathrm{T_f} - \mathrm{T}_{cw}) \quad \textbf{(69)}$$

Heat transfer area of the condenser is obtained by equation (70)

$$\mathrm{Q_c} = \mathrm{U_{LC}}\,\mathrm{A_c}\,\mathrm{LMTD}_c \quad \textbf{(70)}$$

Performance parameters of the MED:

$$\mathrm{PR} = \frac{\mathrm{D}}{\dot{\mathrm{m}}_\mathrm{S}} \quad \textbf{(71)}$$

Specific heat transfer area:

$$\mathrm{sA} = \frac{\sum \mathrm{Aei} + \mathrm{A_C}}{\mathrm{D}} \quad \textbf{(72)}$$

Specific cooling water:

$$\mathrm{sM_{cw}} = \frac{\mathrm{Mcw}}{\mathrm{D}} \quad \textbf{(73)}$$

Economical evaluation of the multi-effect distillation parts is estimated based on correlations provided in literature. DCC of each evaporator and condenser is evaluated as suggested by (Nafey, et al., 2008)

$$\mathrm{DCC} = 430 \times 0.582 \times \mathrm{U} \times \mathrm{A} \quad \textbf{(74)}$$

where U is the heat transfer coefficient in (kW/m^2) and A is the heat transfer area in (m^2). ICC is 20% of the DCC. Annual Capital Cost (ACC) is equal to $\mathrm{TCC} \times \mathrm{A}_F$

Annual Chemical Cost (AChC) in ($/year) is estimated by:

$$\mathrm{AChC} = \mathrm{SChC} \times \mathrm{LF} \times \mathrm{M}_{Distillate} \times 365 \quad \textbf{(75)}$$

SChC (Specific Chemical Cost) is set equal to 0.025 $/m^3$ as suggested by (Sharaf, et al., 2011). Load Factor (LF) is set as 0.9 and $\mathrm{M}_{Distillate}$ is daily water distillate. Similarly, annual Labor Cost (ALC) in ($/year) is equal to:

$$\mathrm{ALC} = \mathrm{SLC} \times \mathrm{LF} \times \mathrm{M}_{Distillate} \times 365 \quad \textbf{(76)}$$

where the specific labor cost is set equal to 0.1 $/m^3$.

Similar to the Annular Electricity Cost (AEC) in solar system, AEC of MED is equal to:

$$\mathrm{AEC} = \mathrm{SEC} \times \mathrm{SPC} \times \mathrm{LF} \times \mathrm{M}_{Distillate} \times 365 \quad \textbf{(77)}$$

Annual Operation and Maintenance Costs (O&M) is 2% of TCC.

Total Annual Cost (TAC) is equal to the summation of the individual annual costs:

$$\mathrm{TAC} = \mathrm{ACC} + \mathrm{AChC} + \mathrm{ALC} + \mathrm{AEC} \quad \textbf{(78)}$$

Hourly cost of the MED desalination system (\$/h) is equal to:

$$Z_{MED} = \frac{TAC + O\&M}{8760} \quad \textbf{(79)}$$

Evaluating MED specific cost of water (\$/m^3) can be done by dividing hourly cost by hourly water production:

$$C_{MED} = \frac{Z_{MED}}{M_{distillate}} \quad \textbf{(80)}$$

4.3 Supplementary Components

Several components are required to complete the Solar-thermal MED desalination system. The components are the burner and the boiler heat exchanger. The objective of the burner is to increase the temperature of the heat transfer fluid if the energy supplied by the solar system is lower than the design temperature. Burner capacity is the maximum thermal power required by the burner which is equal to the thermal power supplied by the solar field and it is mathematically defined as:

$$BurnerCapacity = \frac{Q_{SolarFieldDesign}}{\eta_{burner}} \quad \textbf{(81)}$$

where η_{burner} is equal to 90%.

The amount of energy supplied by the burner ($Q_{Auxiliary}$) is equal to:

$$Q_{Auxiliary} = Q_{SolarFieldDesign} - Q_{Solar} \quad \textbf{(82)}$$

If $Q_{Solar} > Q_{SolarFieldDesign}$ then some of the collectors will be de-focused to maintain the outlet temperature.

Solar share is defined as the ratio of solar thermal energy to the total thermal energy required by the system.

$$SolarShare = \frac{Q_{Solar}}{Q_{Solar} + Q_{Auxiliary}} \quad \textbf{(83)}$$

The second supplementary component is the boiler heat exchanger. The objective of the boiler is transferring the heat collected by the heat transfer fluid from the solar

collector and the burner to the water circuit to derive the MED desalination system. Thermal power of the boiler is determined by the heating power required by the MED.

$$Q_{Boiler} = \frac{Q_{MED}}{\eta_{boiler}} \quad \textbf{(84)}$$

Heat transfer area of the boiler can be calculated using equation (85)

$$\mathrm{Q}_{Boiler} = \mathrm{U}_{Boiler}\, \mathrm{A}_{Boiler}\, \mathrm{LMTD}_{Boiler} \quad \textbf{(85)}$$

Economical estimation of the supplementary components is as follows:

Cost of the burner is estimated as proposed by (Palenzuela, et al., 2015)

$$DCC_{Burner} = 60 \times BurnerCapacity \quad \textbf{(86)}$$

ICC is estimated as 20% of the DCC and O&M cost is 15% of the TCC.

Unit cost of fuel equal to 1.84 $/GJ is used to obtain the cost of fuel.

DCC of boiler heat exchanger is estimated using the correlation provided by (Nafey, et al., 2008):

$$\mathrm{DCC} = 1000 \times (12.86 + \mathrm{A}^{0.8}) \quad \textbf{(87)}$$

MED-Solar thermal design is based on steady state operation of MED system under fixed conditions because of the difficulty in unsteady operation of MED system.

Therefore, auxiliary heater is used to guarantee steady state operation. No thermal storage is used because of the high cost which producing non-economic system.

The followed design methodology for MED-Solar thermal is as follows:

1. MED desalination plant is designed based on the water demand capacity.
2. Thermal power required to operate the MED plant is evaluated.
3. Solar field is designed based on the required thermal power and design solar irradiation (I_{Design}). Three I_{Design} are implemented in this study, yearly maximum solar irradiation, yearly average solar irradiation and yearly day-average solar irradiation (excluding night hours). The description of the three design solar irradiation and their values for Dhahran, Saudi Arabia are summarized in Table 14.
4. Using hourly solar irradiation (I), heat transfer fluid's (HTF) outlet temperature is evaluated. If I is greater than I_{Design}, some of the collectors are turned off to maintain thermal power delivery.
5. Auxiliary heat is required if I is less than I_{Design} to maintain the HTF temperature at the design temperature. Auxiliary burner is used with natural gas.
6. Performance parameters and cost estimation of the MED-Solar thermal system are calculated.

The presented methodology is shown in Figure 24. The parameters at which the analysis is performed are shown in Table 15.

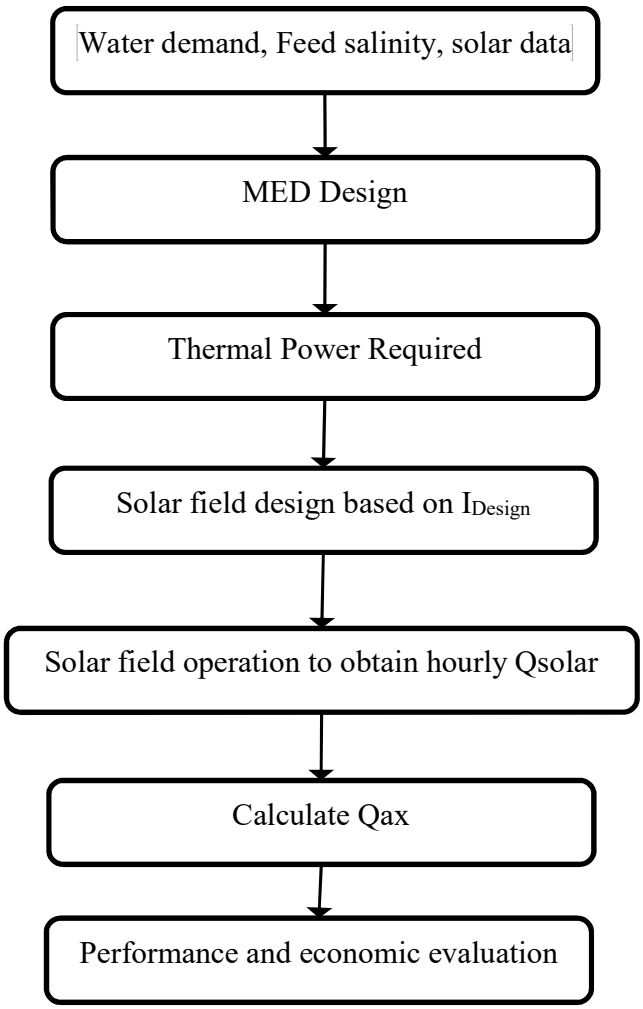

Figure 24: Design Methodology of MED-Solar thermal

Table 14: Description of the implemented I_{design} and their values for Dhahran, Saudi Arabia

Idesign	Description	I (W/m2)
I_{max}	Yearly maximum solar irradiation	991.8
$I_{avg,day}$	Yearly average solar irradiation over days only (excluding night hours)	464.3
I_{avg}	Yearly average solar irradiation	232.2

Table 15: Design parameter of MED-Solar thermal

Parameter	Value
$M_{distillate}$	1000 m^3
T_{cw}	25 C
T_f	35 C
T_s	75 C
X_f	42,000 PPM
X_B	70,000 PPM
No. of effects	8
Collector type	LS-2
Heat Transfer Fluid	Therminol VP1
Fuel	Natural gas

CHAPTER 5

RESULTS AND DISCUSSION

Results and discussion is divided into two sections. One is for renewable energy membrane desalination systems and the other is for renewable energy distillation systems.

5.1 RE Membrane Desalination Systems

The presented methodology of RO-PV and RO-Wind in Chapter 3: Membrane Desalination Systems including thermo-economic models of solar photovoltaic, wind and reverse osmosis are implemented in Engineering Equation Solver (EES) software package.

To illustrate the application of the methodology, different cases for RO-Wind and RO-PV are analyzed and compared for the city of Dhahran, Saudi Arabia. For RO-Wind, six different cases are presented in Table 16 to show different scenarios. The first four cases have the same power system size and desalination system size. Therefore, average water production in each month is the same for these cases as shown in Figure 25. They differ only in the operation starting month. Although the methodology introduced guarantee that average water production is more than water demand, status of the storage tank should be considered to also guarantee continuous supply of desalinated water especially in the first years. Figure 26 shows the status of

the storage tank at the end of each month for the six cases. Status of the water tank is strongly dependent of the starting month and therefore it should be carefully considered, otherwise larger desalination system –and may be power system- will be needed to satisfy the continuous supply of water. Beginning the desalination process from January (Case 1) is good enough in this case since water is available throughout the year. January is a good month to start with since its average wind speed is higher than the yearly average wind speed and it is followed by months of also higher wind speed than the average i.e. February and March. This helps water to accumulate in the tank to be used in months with lower wind speed and lower water production as a result. Status of the tank for the first year for Case 1 can be seen in Figure 26.

Table 16: Six different cases of RO-Wind

	Case 1	Case 2	Case 3	Case 4	Case 5	Case 6
Daily Water Demand (m^3)	1,000					
Daily Average Water Production (m^3)	1,027	1,027	1,027	1,027	1,090	1,148
Starting Month	January	February	June	November	February	June
# of Turbines	6	6	6	6	6	6
# of Pressure Vessels	10	10	10	10	11	12
# of Storage Tanks	3	3	3	3	4	6
Water Specific Cost ($/$m^3$) (based on water production)	1.366	1.366	1.366	1.366	1.395	1.471
Water Specific Cost ($/$m^3$) (based on water demand)	1.403	1.403	1.403	1.403	1.521	1.689

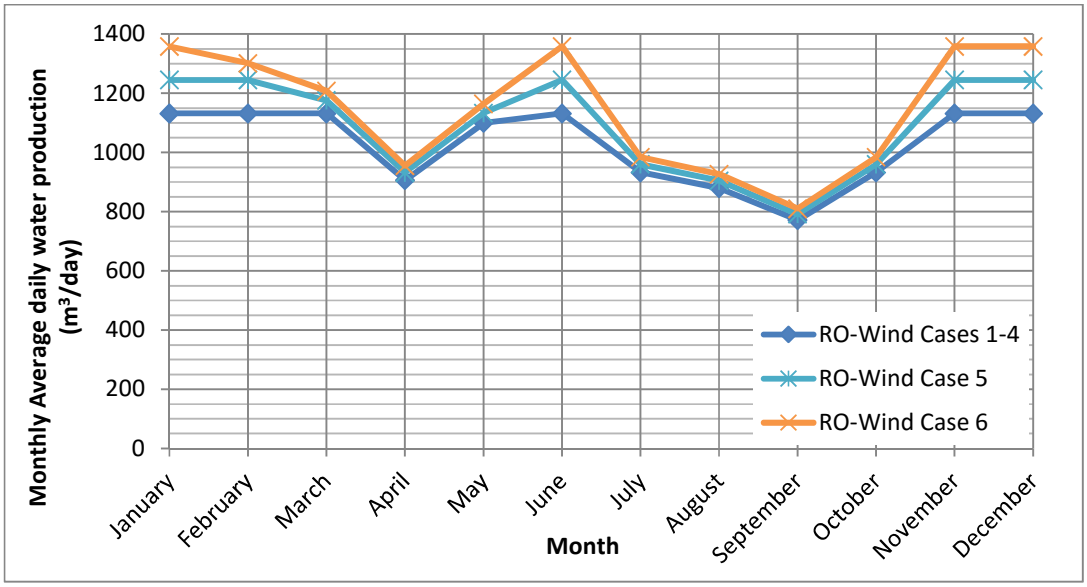

Figure 25: Monthly Average Daily Water Production for six cases of RO-Wind

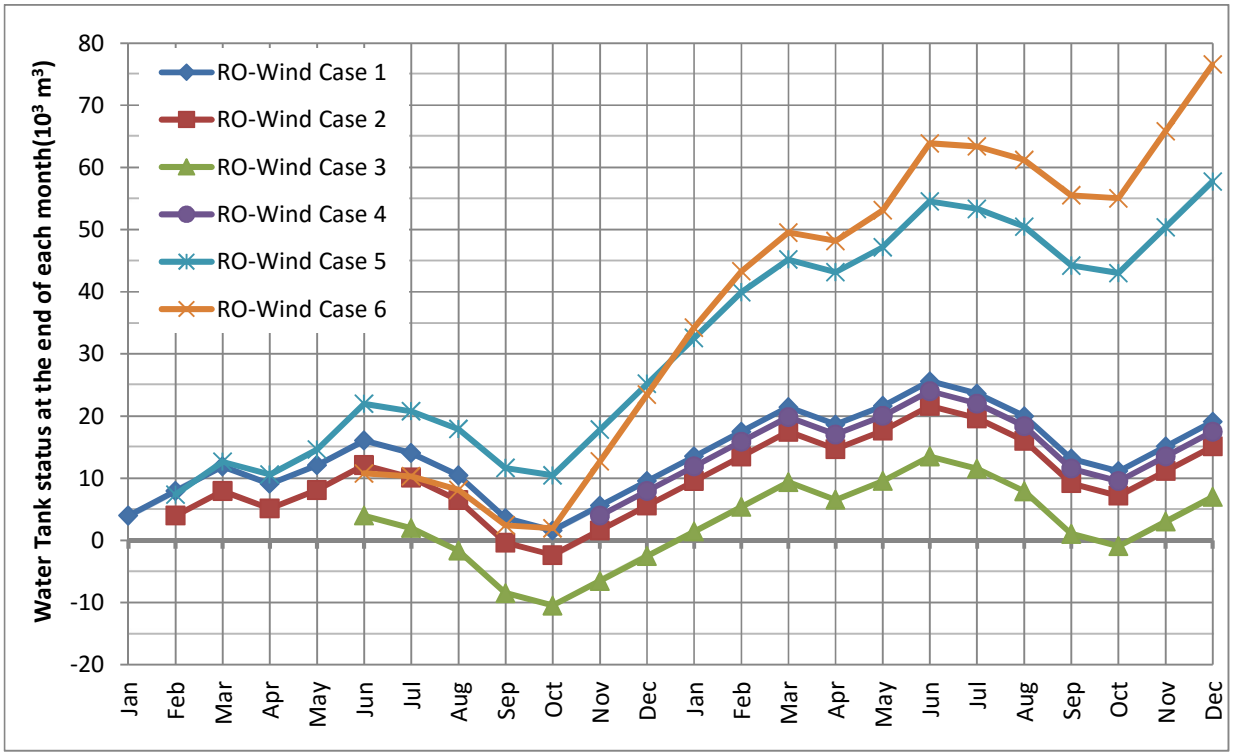

Figure 26: Water Tank Status at the end of each month for six cases of RO-Wind

Starting the operation in February (Case 2) is not preferred choice because we will reach to a point where water demand is more than water available on September and October. To overcome this issue, the code will size up the RO plant by one additional pressure vessel. This will result in increasing average water production as seen in Figure 25 and Figure 26 for Case 5. As a result, number of storage tanks and water specific cost based on total water demand are increased. Specific cost based on water production is reduced because no additional wind turbines are needed so the reduction

in specific cost of power system is more than the increment in specific cost of desalination and storage systems.

Starting the operation in June (Case 3) seems to be attractive since it has the maximum wind speed but because it is followed by four months of lower wind speed which will result in running out of the water. In fact, June is one of the worst months in starting the operation and two pressure vessels are required to satisfy the demand. Case 6 in Figure 25 and Figure 26 is representing the modification of Case 2.

Case 4 is representing the starting operation in November. It is observed that water is available in storage tanks throughout the year. It can be approved that for Dhahran, November is the best month to start the operation because it is the first month in consecutive months of wind speed higher than the average, i.e. December, January, February and March.

In applying the proposed methodology, selection of the starting month is important and it should go through careful study. It is location property and November is the best month for Dhahran. Therefore, November is selected to be the starting month in wind power throughout this study.

Similar analysis is applied for RO-PV. Five cases of RO-PV are presented in Table 19 to show differences caused by the selection of the starting month. Monthly average daily water production and water tank status for the five cases could be seen in Figure

27 and Figure 28 respectively. Best selection is April since it is the first month in consecutive months where monthly average daily radiation is higher than yearly average daily radiation. Having global radiation more than the average means producing desalinated water more than the demand. Therefore, April is selected to be the starting month for solar PV throughout this study. Again, June seems to be attractive since it has the maximum solar radiation but tracking the storage tank status we can see that water supply is less than the demand in February. Adapting the size of RO system by adding one pressure vessel is enough to guarantee continuous supply of desalinated water. January case (Case 3) is one of the worst months because its average solar radiation is less than the yearly average and since it is the first month and no water is available in the tanks so both power system and desalination system should be enlarged. Case 5 is presenting the design of the systems if January is the starting month. Number of PV panels are increased from 8778 to 10698 and pressure vessels are increased from 27 to 39. Although the increment in specific cost is only 35 cents but the water produced is much more than the demand and this is clear from the storage tank volume required.

Table 17: Five different cases of RO-PV

	Case 1	Case 2	Case 3	Case 4	Case 5
Daily Water Demand (m^3)	1000				
Daily Average Water Production (m^3)	1016	1016	1016	1032	1316
Starting Month	April	June	January	June	January
# of PV Panels	8778	8778	8778	8778	10698
# of Pressure Vessels	27	27	27	28	39
# of Storage Tanks	3	3	3	3	12
Water Specific Cost ($/$m^3$) (based on water production)	2.119	2.119	2.119	2.115	2.466
Water Specific Cost ($/$m^3$) (based on water demand)	2.153	2.153	2.153	2.183	3.245

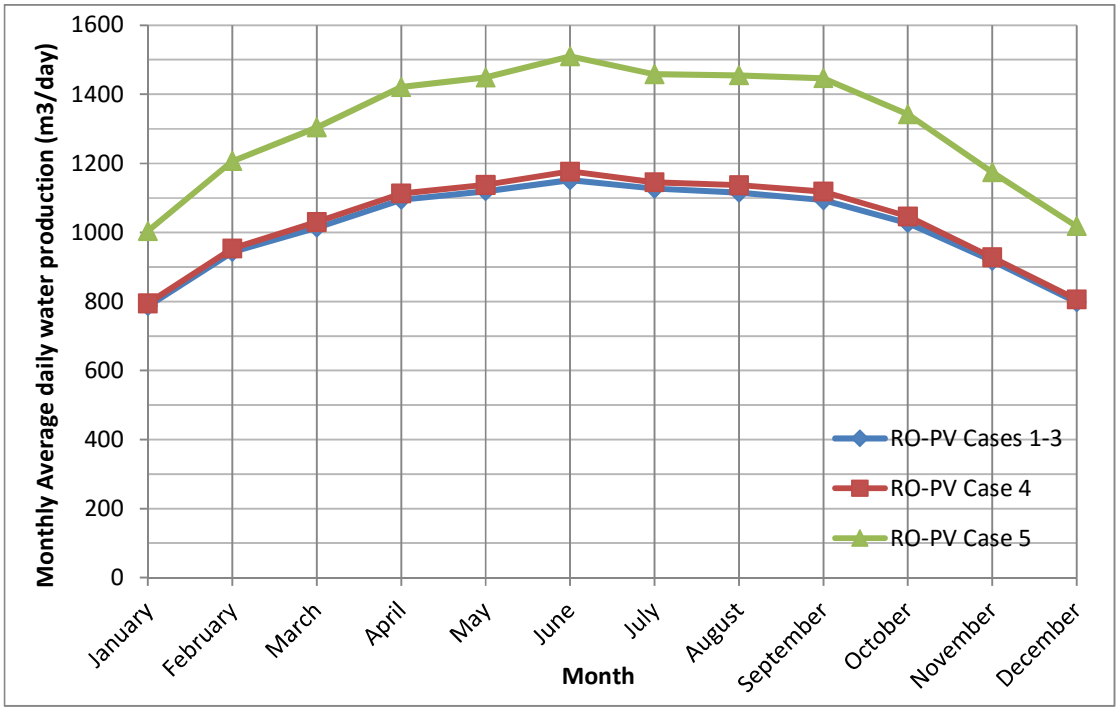

Figure 27: Monthly Average Daily Water Production for five cases of RO-PV

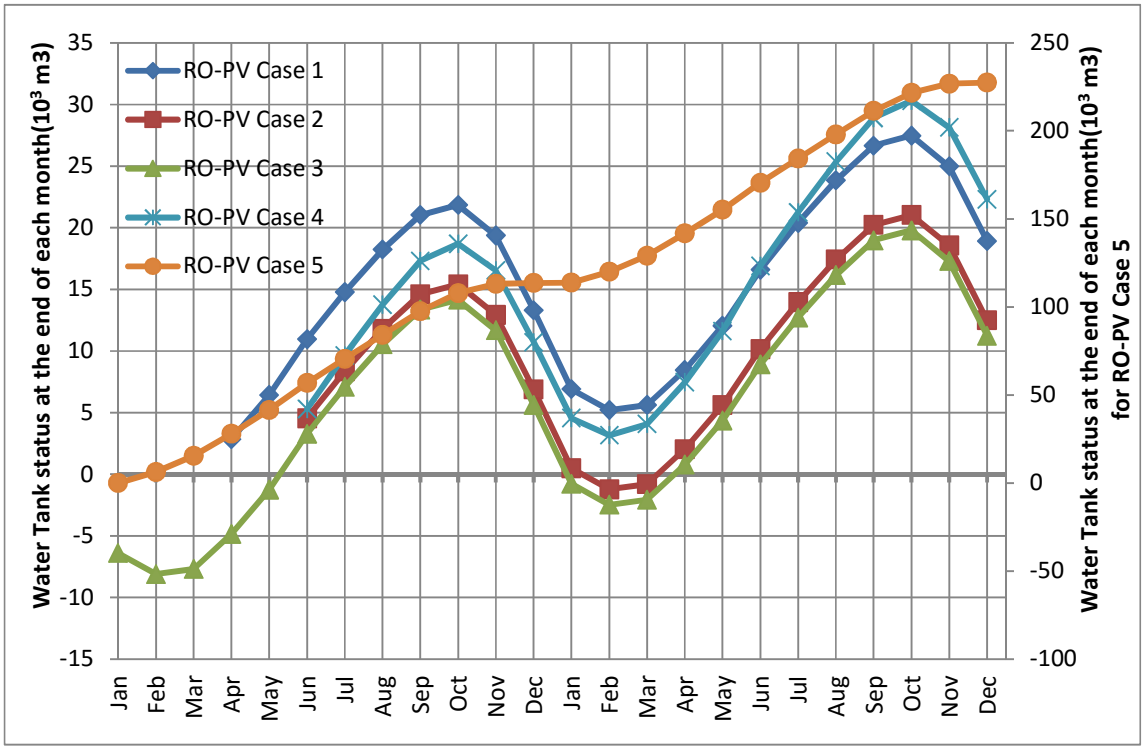

Figure 28: Water Tank Status at the end of each month for five cases of RO-PV

In comparing the specific cost between Case 1 and Case 4 we can observe that it is decreased because the power and storage systems' specific costs are reduced due to the increased production. However, specific cost of desalination system is increased. In the comparison between Case 1 and Case 5 we can see that the net cost increment is 0.347 $ per cubic meter. This is caused by the increment of specific cost of RO and storage systems, although, the specific cost of power system is reduced due to full utilization of power produced. Cost comparisons are presented in Table 18. Although two specific costs are presented in Table 16 and Table 17, one is based on water

production and one is based on water demand, specific cost based on water production is used throughout this thesis because it is representing the actual cost of water.

Table 18: Cost Comparison between Cases of RO-PV

Specific Cost ($/m^3)	Case 1	Case 4	Case 5
Power System	0.6892	0.6781	0.6483
Desalination System	1.270	1.279	1.324
Storage System	0.1599	0.1573	0.4983
Total	2.119	2.115	2.466

Sometimes the concept of sizing up the desalination and/or power systems is not practical solution. Therefore, we could look at it from another point of view which is how long the period required to reach steady state water availability where water will be available in the storage tanks throughout the year. The required period is expressed in years and depend strongly on the operation starting month. The case of RO-PV is presented in Table 19. The period required to reach steady state water availability for different cases of operation starting month is shown in Table 20. The table shows that

if the operation starts from January, the steady state water availability will be only reached by the third year. During the first two years, supplementary water source should be used to guarantee continuous water supply to the community. The steady state water availability will be obtained from the first year if the operation starts from April since it is the first month in consecutive months where monthly average daily radiation is higher than yearly average daily radiation. Having global radiation more than the average means producing desalinated water more than the demand. Therefore, April is selected to be the starting month for solar PV throughout this study.

Table 19: Results of the Case of RO-PV

Quantity	#
Daily Water Demand (m^3)	1,000
Daily Average Water Production (m^3)	1,016
# of PV Panels	8,778
# of Pressure Vessels	27
# of Storage Tanks	3
Water Specific Cost ($/$m^3$) (based on water production)	2.119
Water Specific Cost ($/$m^3$) (based on water demand)	2.153

Table 20: Steady state water availability period required for different cases of operation starting month of RO-PV

Operation Starting Month	Steady state water availability reached by:
January	Third Year
April	First Year
June	Second Year
November	Forth Year

Cost of water by wind is less than cost of water by solar. For daily average water demand of 1,000 m^3, cost of water in RO-Wind (Case 4) is 1.366 \$/m^3 while in RO-PV it is 2.119 \$/m^3. Table 21 shows that number of pressure vessels in RO-PV is almost three times number of vessels needed in RO-Wind for the same water capacity. In addition, amount of power installed in RO-PV system is 80% more than the amount of power installed in RO-Wind. These two factors impose RO-PV cost to be more than RO-Wind cost by 55%. This shows that the main reasons behind this difference are the larger amount of installed power and the larger desalination system (or storage systems in case of energy storage) caused by the long-time off-operation during night.

Table 21: Comparison between RO-Wind and RO-PV

Quantity	RO-Wind	RO-PV
Daily Water Demand (m^3)	1,000	
Daily Average Water Production (m^3)	1,027	1,016
# of turbines/panels	6	8,778
# of Pressure Vessels	10	27
# of Storage Tanks	3	3
Specific Cost of Power System ($/$m^3$)	0.2675	0.6892
Specific Cost of Desalination System ($/$m^3$)	0.9406	1.270
Specific Cost of Storage System ($/$m^3$)	0.1582	0.1599
Water Specific Cost ($/$m^3$) (based on water production)	1.366	2.119

Previous analysis was obtained under fixed feed water concentration of 45,000 PPM. Similar methodology is applied for different feed water concentration. Figure 29 shows the specific cost of water produced by RO-Wind and RO-PV at feed water concentration ranging from 25,000 PPM to 60,000 PPM where the average water demand is fixed as 1,000 m^3/day. It is observed that the cost is increased exponentially in both combinations as the feed water concentration increased. Also, as noted, the

difference between cost of water by RO-PV and cost of water by RO-Wind is increasing from 0.52 $/m^3 for 25,000 PPM to 1.019 $/m^3 for 60,000 PPM.

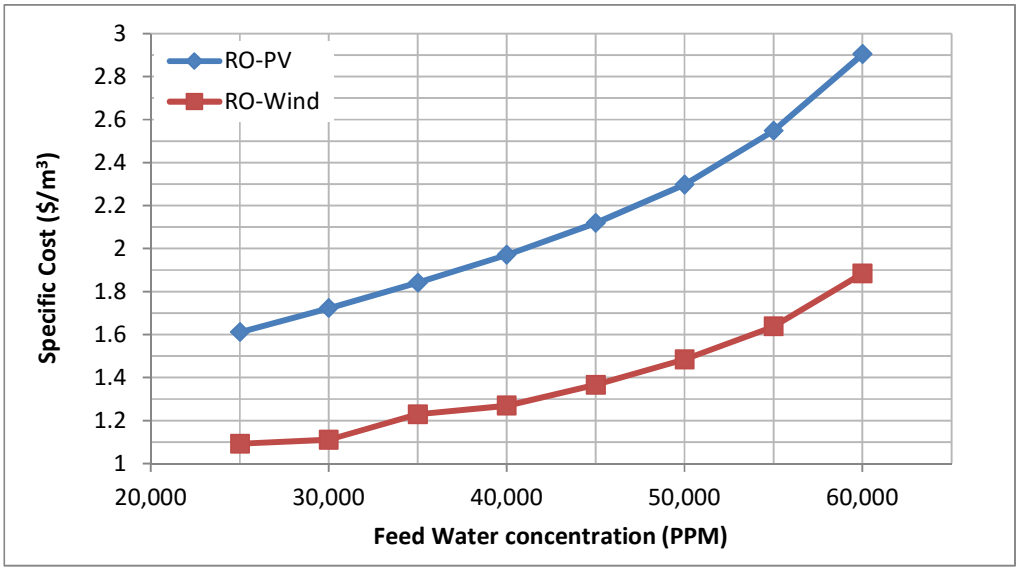

Figure 29: Water Cost for system daily capacity of 1,000 m^3 using RO-Wind and RO-PV at different feed water concentration

It is highly important to study water cost at different system sizes. Based on the concept of scale, cost is expected to decrease as the size increases. Figure 30 present water cost at different daily average water demand using both techniques, RO-Wind and RO-PV. As expected, cost is decreasing as the capacity increases. The difference in cost between RO-PV and RO-Wind is almost 0.72 $/m^3 for all cases. As explained, larger RO plant required in PV is mainly the reason behind this difference. As seen in

Figure 31 and Figure 32, number of storage tanks is exactly the same for both combinations while number of pressure vessels in PV is 2.5 multiple of pressure vessels in Wind.

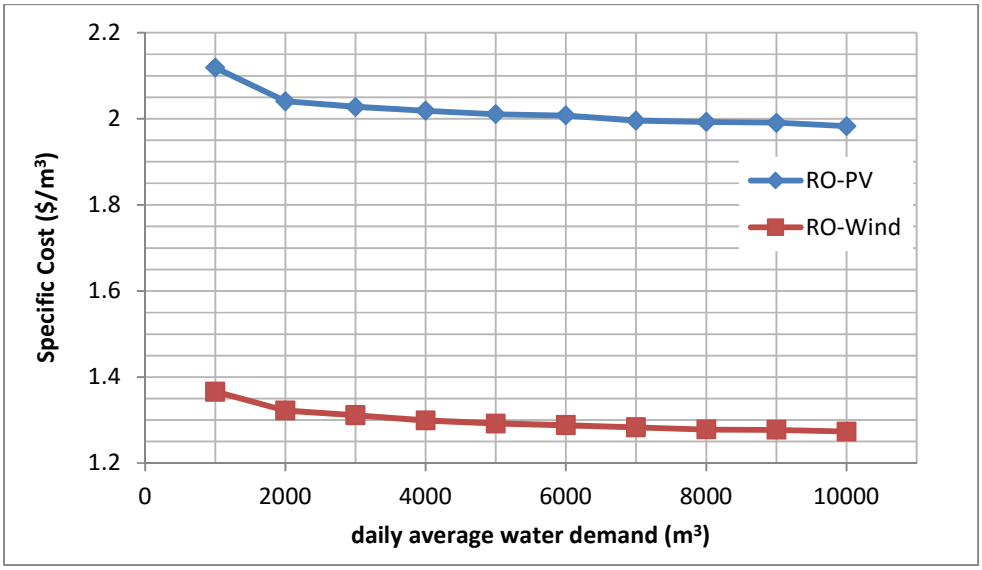

Figure 30: Cost of water produced by RO-Wind and RO-PV at different water demand capacity

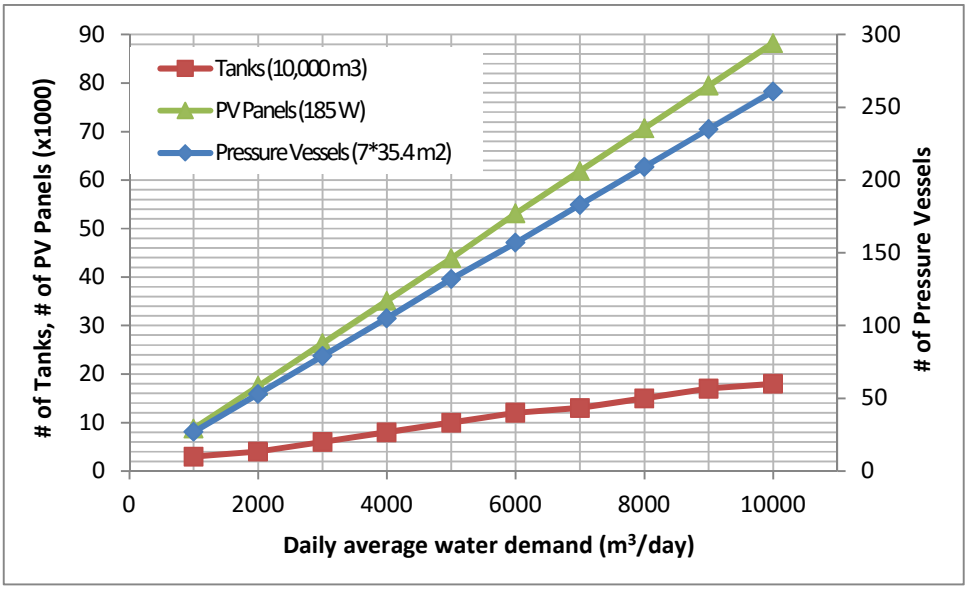

Figure 31: Number of pressure vessels, storage tanks and wind turbines used at different system capacity

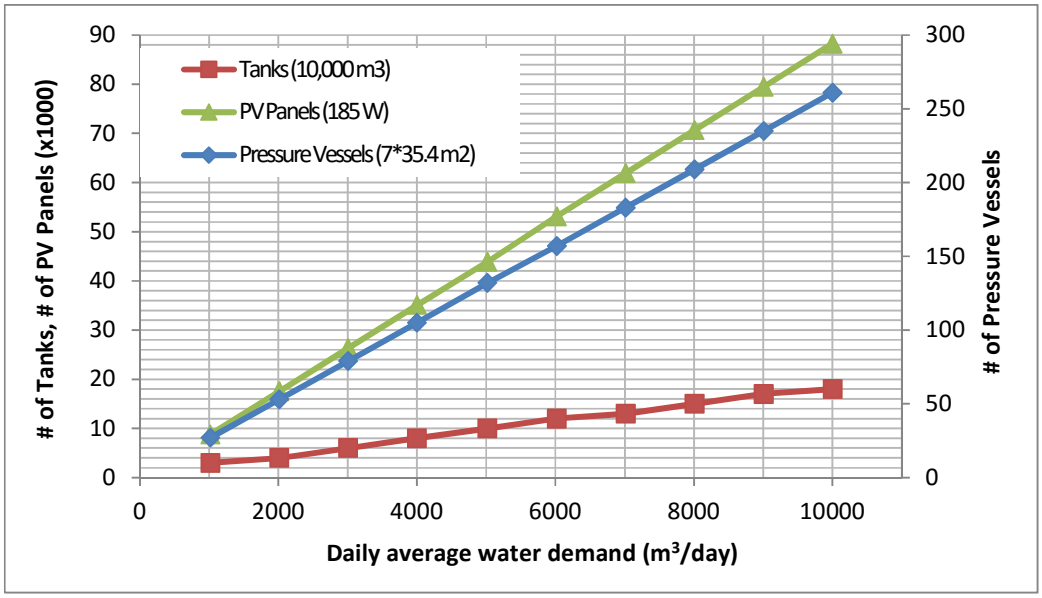

Figure 32: Number of pressure vessels, storage tanks and PV panels used at different system capacity

It is very important to consider safety factor in the design of desalination plants. The importance of safety factor is to overcome any sudden reduction in water availability caused by sudden or planned shutdown of the plant or due to drastic weather changes. Safety factor in this study is expressed as a percentage of water demand. The system size is determined based on the overall water demand including the additional amount considered as a safety factor. Figure 33 shows cost of water for plant capacity of 10,000 m^3 per day for the two systems of RO-Wind and RO-PV. Cost of water reduces slightly as the safety factor increases. For RO-Wind, the cost reduces from 1.273 $/$m^3$

for the basic system with zero safety factor to 1.262 $/m^3 for the system with 50% safety factor. Similar behavior is observed for RO-PV.

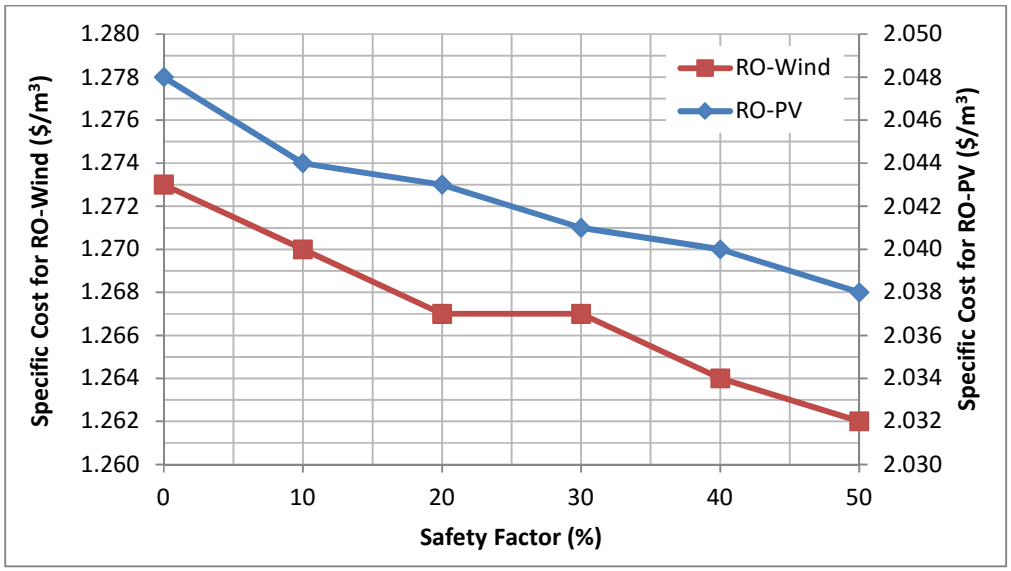

Figure 33: specific cost of water at different safety factors for system capacity of 10,000 m^3 per day.

5.2 RE Distillation Systems

Similar analysis to RO-Wind and RO-PV is done for MED-solar thermal. The basic design parameter and results are illustrated in Table 22. Cost of such a system is breaking down mainly into cost of MED system and solar system in addition to fuel cost and supplementary systems. Solar energy collected by the solar field for typical days in four months are presented in Figure 34. We can see from the figure that the system is not operated solely by solar unlike RO-PV and RO-Wind systems in which operated 100% by renewable energy. Solar share for this case is around 24.4 %. To increase solar share, we could decrease I_{Design} to obtain larger solar collector system and, as a result, capturing more solar energy. However, on the other side, if solar irradiation is more than I_{Design}, some of the solar energy will not be captured due to the limitation in MED system. Two additional I_{Design} were studied to see the effect on solar collector size, solar share, specific and total costs. Implemented I_{Design} values were discussed in Table 14. Results of different cases are presented in Table 23. It is clear from the table that larger solar collector is used and therefore more solar energy is captured. This can be seen clearly from Figure 35 and Figure 36 for I_{Design} equal to 464.3 and 232.2 W/m^2, respectively.

Table 22: Design Parameter and Results of MED-Soalr combination

Parameter	Value	Unit
M_demand	1000	M^3/day
ϕ	26.1	degrees
X_feed	45000	PPM
I_{Design}	I_{max}=991.8	W/m2
Specific cost of MED sub-system	0.9982	$/m3
Specific cost of solar sub-system	0.5529	$/m3
Specific cost of MED-solar thermal	2.282	$/m3
Solar collector length	61.54	M
Solar collector rows	23	#

Table 23: Results of three cases at different I_{Design}

I_{Design}	I_{max} (991.8 W/m^2)	$I_{avg,day}$ (464.3 W/m^2)	I_{avg} (232.2 W/m^2)
M_{demand}	1000		
X_{feed}	45000		
I_{design} (W/m2)	991.8	464.3	232.2
Collector length (m)	61.54	131.3	264.9
Solar Share (%)	24.37	37.5	43.29
Specific cost of MED sub-system ($/m3)	0.9982	0.9982	0.9982
Specific cost of solar sub-system ($/m3)	0.5529	1.051	1.93
Specific cost of MED-solar thermal ($/m3)	2.282	2.716	3.625

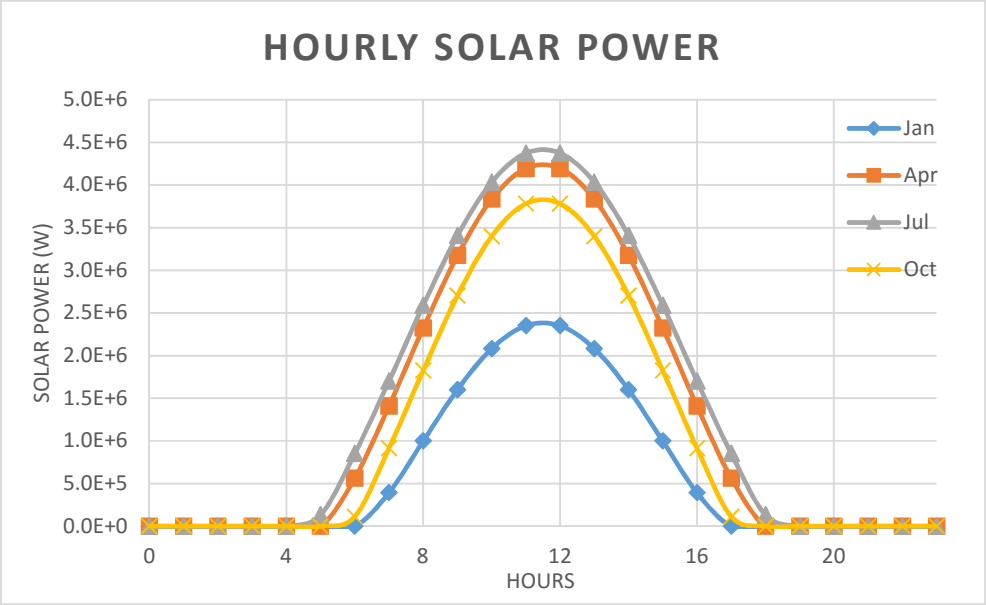

Figure 34: Solar filed collected energy over the day in typical four months for $I_{design}=I_{max}$ (Water demand=1000 m^3/day, Feed Concentration=45000 PPM)

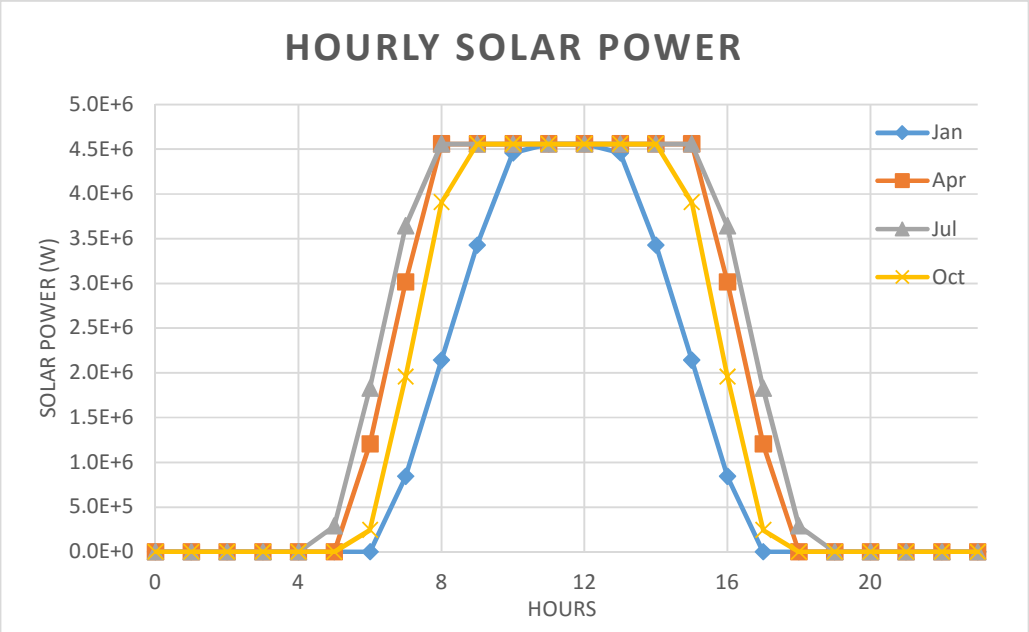

Figure 35: Solar filed collected energy over the day in typical four months for $I_{design}=I_{avg,day}$ (Water demand=1000 m^3/day, Feed Concentration=45000 PPM)

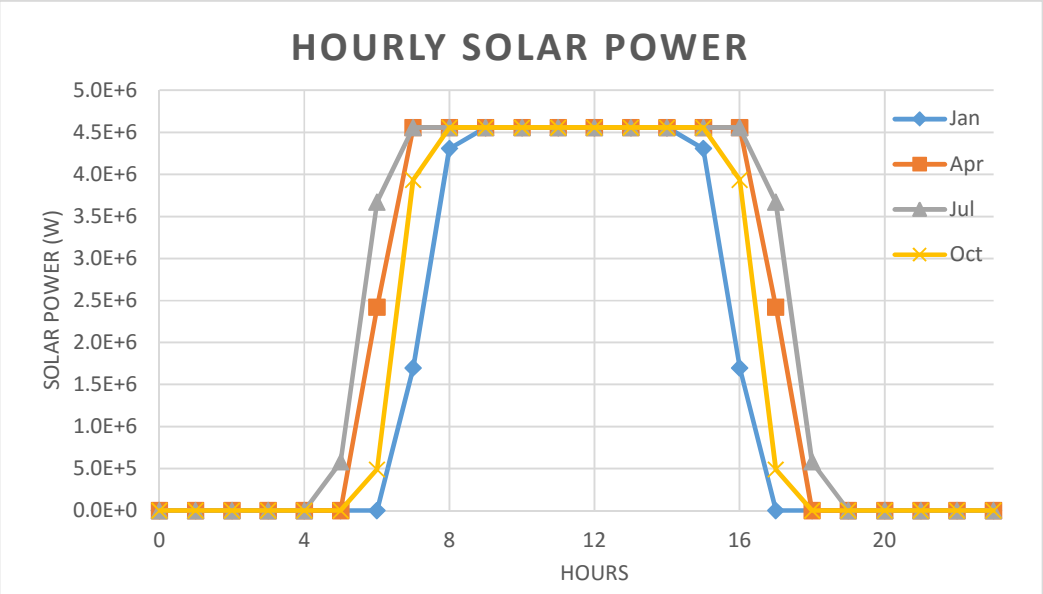

Figure 36: Solar filed collected energy over the day in typical four months for $I_{design}=I_{avg}$ (Water demand=1000 m^3/day, Feed Concentration=45000 PPM)

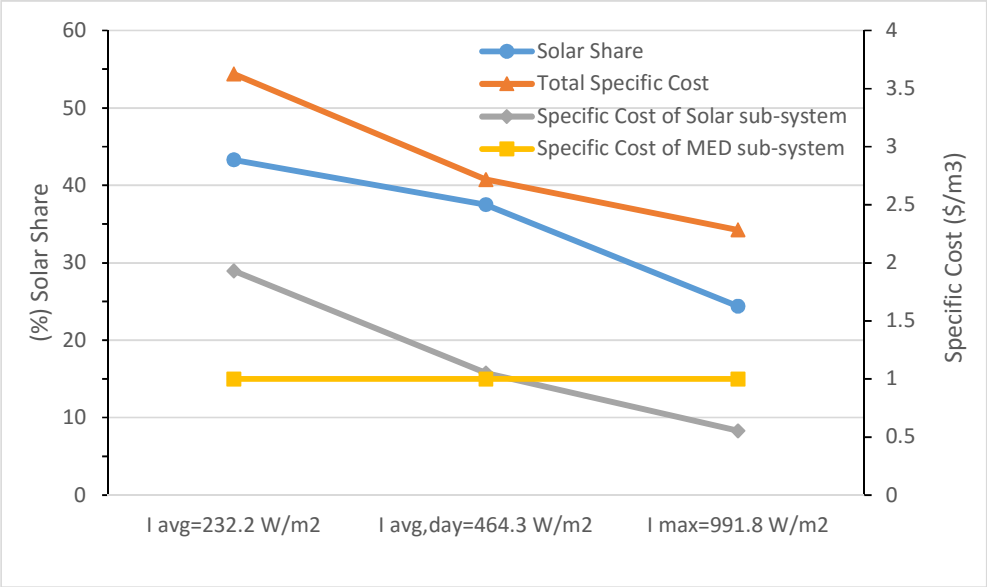

Figure 37: Variation of specific costs and solar share with I_{Design}

Figure 35-Figure 37 showed that as we decrease the design solar irradiation, more solar energy will be captured due to larger solar field which lead to higher solar share. Therefore, I_{Design} could be selected to obtain targeted solar share of the solar system.

Solar field size is characterized by the number of rows and the length of each row. Both of these parameters are identifying the amount of energy captured from the solar field at design irradiation. While the number of rows is defined by the amount of flow rate of the Heat Transfer Fluid (HTF), the length of each row is defined by HTF design outlet temperature. Figure 38 shows number of rows and length of solar field at variable desalination capacity and design solar irradiation. It can be seen that number of rows is affected by plant capacity and not by design solar irradiation. The figure

shows identical curves for the three I_{Design}. On the other side, length of the solar collector is function of I_{Design}. However, capacity of the plant is not affecting the length of the collector, as expected.

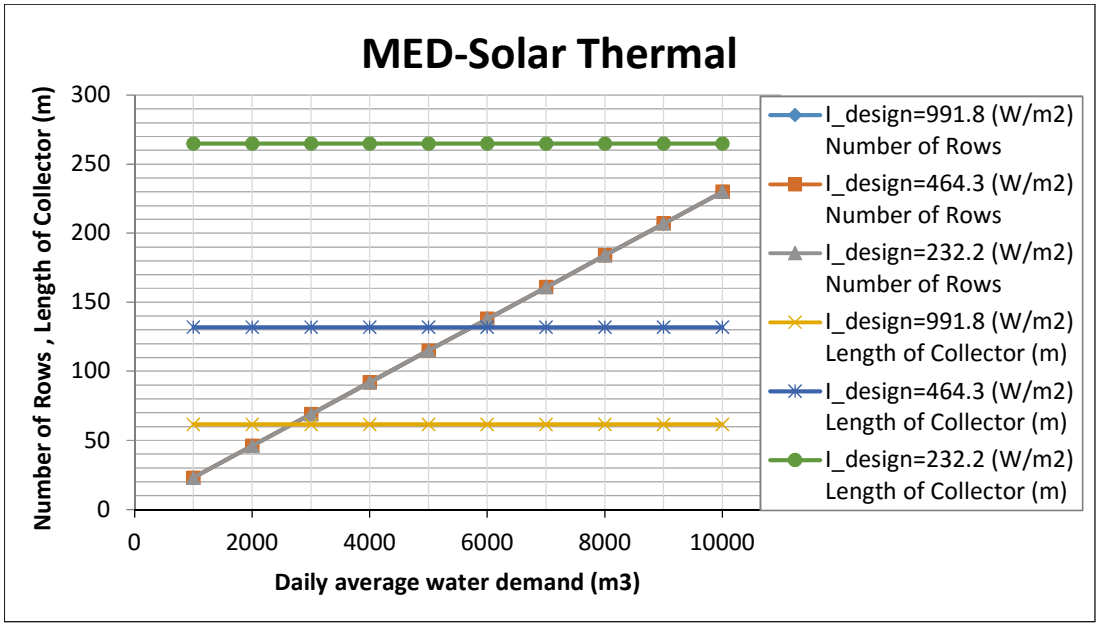

Figure 38: Number of rows and length of solar collector at different desalination capacity and design solar irradiation.

Solar share increases from 24.4% to 43.3% for I_{Design} 991.8 to 232.2 W/m^2, respectively. However, the specific cost of solar field increases from 0.553 to 1.93 \$/m^3 while the specific cost of desalination system is the same because no changes to the desalination system. This increase leads to 60% increase in total cost. Such design of MED-Solar system is not economically feasible.

Cost estimation for different conditions such as different feed water concentration, daily water demand and safety factor are presented in Figure 39, Figure 40 and Figure 41, respectively, for the three presented I_{Design}.

It is clear from Figure 39 that as feed water concentration increases, cost of water increases as well. However, as expected, cost of water decrease as water production increases as presented in Figure 40. Figure 41 highlights the importance of safety factor in design and it shows that the cost of water is decreasing as safety factor increases. The definition of safety factor here is exactly the same as the presented in RO-PV and RO-Wind which is percentage of water demand.

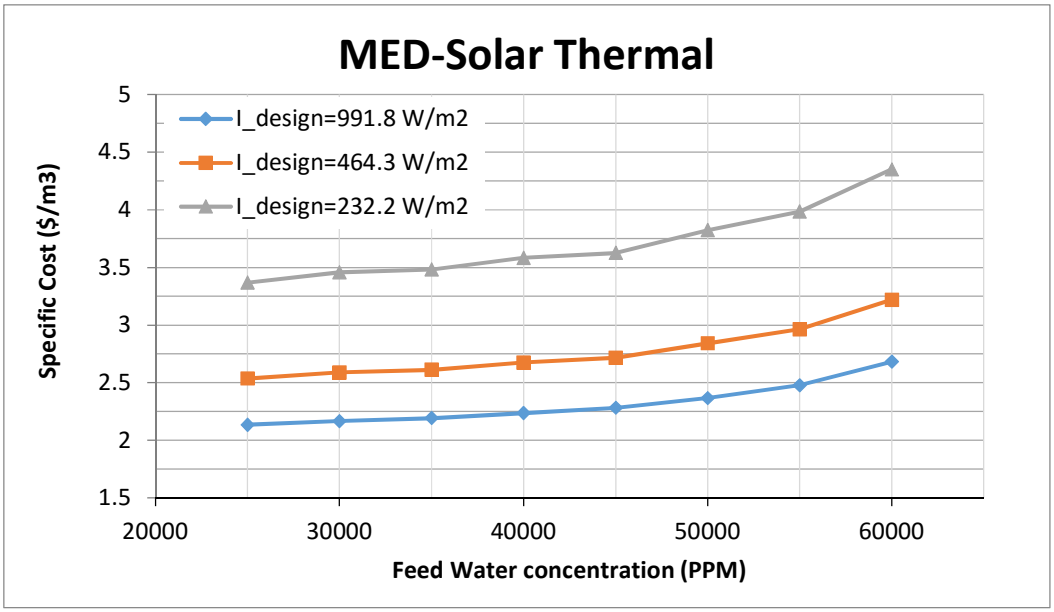

Figure 39: Cost estimation of MED-Solar as a function of Feed water concentration

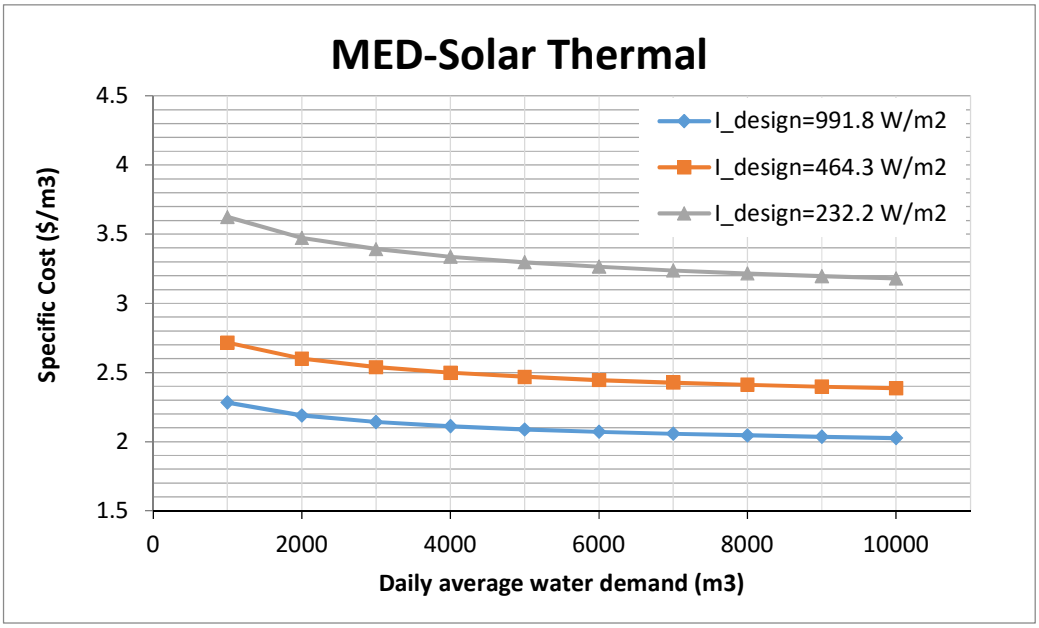

Figure 40: Cost estimation of MED-Solar as a function of daily water demand

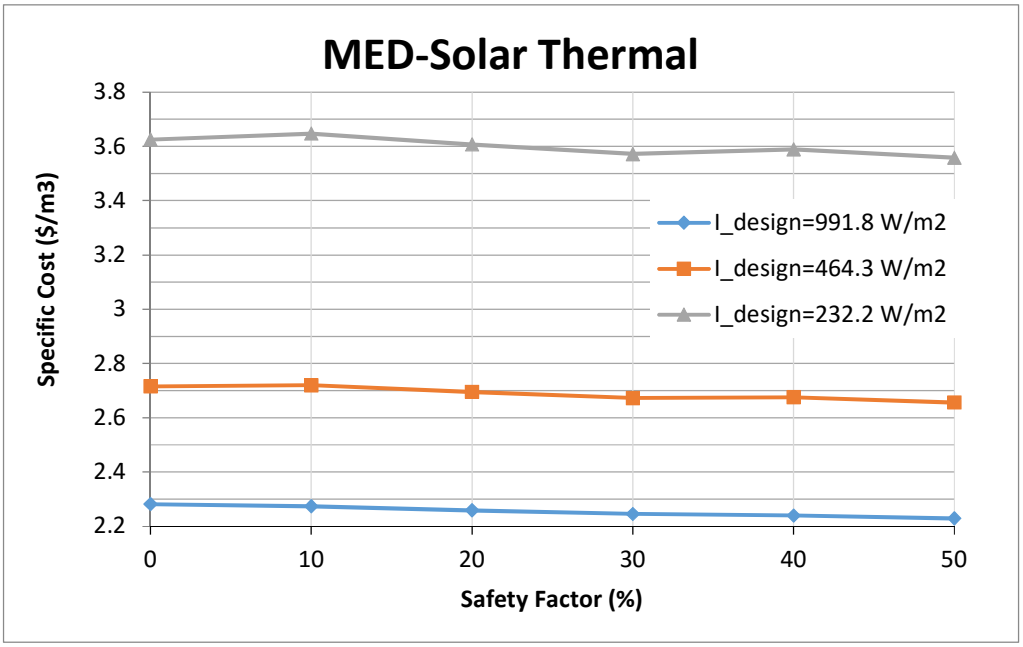

Figure 41: Cost estimation of MED-Solar as a function of safety factor at daily water demand of 1000 m^3

5.3 Overall Comparison of RE Systems

To simplify cost comparison between the three combinations (RO-Wind, RO-PV and MED-Solar), Figure 42 shows the cost of these technologies for daily water demand from 1000 m^3 to 10000 m^3 and feed water concentration of 45,000 PPM for the city of Dhahran. The figure shows that RO-Wind is the cheapest whereas MED-Solar is the most expensive. It is also notable here that the rate of cost decreasing of MED-Solar is higher than the others and it is becoming competitive to RO-PV at high system capacity. One of the main differences between the three combinations is that RO-Wind and RO-PV are 100% renewable while Solar-MED is only 24-25% renewable

for the considered design irradiation. Higher renewable share is expected for lower design irradiation but also higher cost. Figure 43 shows the cost of the three combination for a system capacity of 1000 m^3 for the city of Dhahran at different feed water concentration. The figure shows that RO-Wind combination is the cheapest. RO-PV combination is the second cheapest for feed water concentration below 52,000 PPM, however, at feed water concentration above 52,000 PPM, MED-Solar thermal is the second cheapest. This is caused by the lower sensitivity of feed water concentration in MED-Solar unlike RO-PV and RO-Wind. This sensitivity is represented here by the lower rate of change in MED-Solar. Out of the three MED-Solar configurations discussed in Section 5.2 (RE Distillation Systems), only the case of I_{Desgin} =991.8 W/m^2 is used in the aforementioned comparison because its cost is the lowest out of the three which makes it the most competitive to RO-PV and RO-Wind.

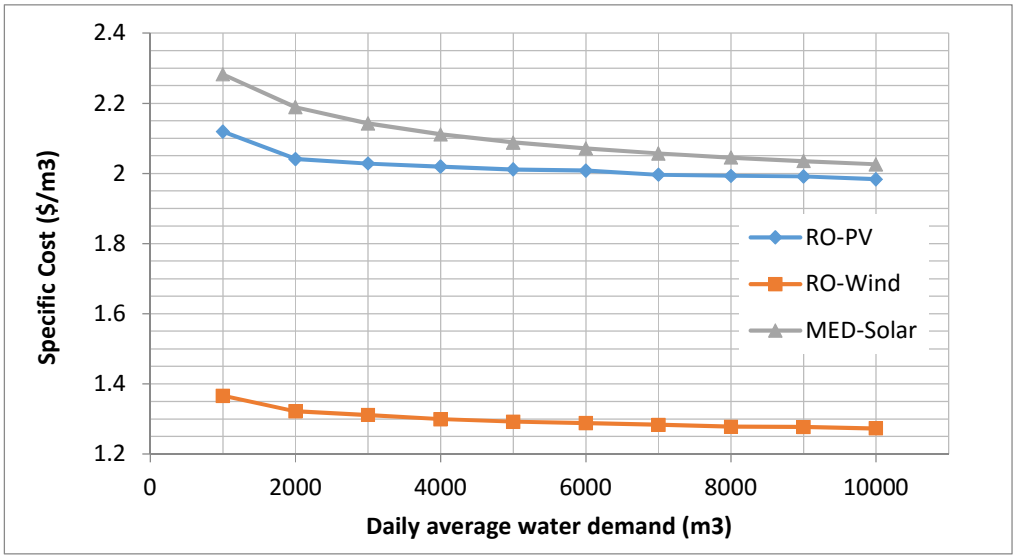

Figure 42: Cost estimation of the three systems at different water demand for feed water concentration of 45,000 PPM

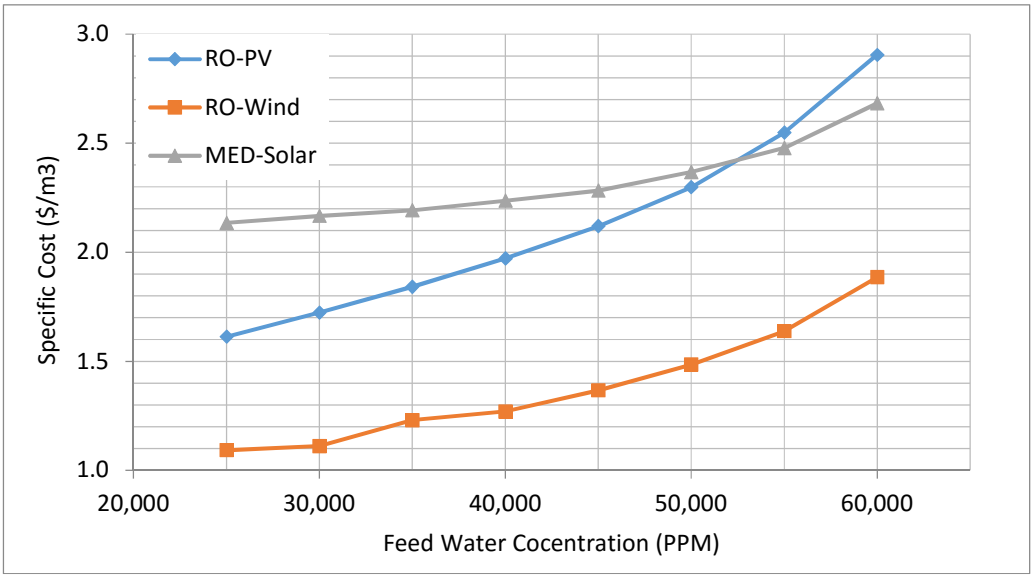

Figure 43: Cost estimation of the three systems at different water demand for a system capacity of 1000 m^3

5.4 Analysis for cities of Saudi Arabia

Specific cost comparison between the three analyzed technologies for different cities across the kingdom of Saudi Arabia is presented in this section. Three coastal cities, in addition to Dhahran, are selected. These are Jubail, Yanbu and Jeddah. These cities contain most of the desalination plants in the kingdom. Data of these cities are collected from NASA Atmospheric Science Data center and RETScreen software provided by Natural Resources Canada. Data are given in APPENDIX.

Cost depend strongly on the availability of renewable resources; therefore, we can see that the optimum selection differs from one city to another. Figure 44 shows the cost

of water production by the three configurations in the aforementioned cities for system capacity of 1000 m^3 per day and feed water concentration of 45000 PPM. We can see that RO-Wind is the optimum selection in Dhahran and Jubail (Eastern Province) while RO-PV is the optimum selection in Jeddah and Yanbu (Western Province). However, MED-Solar is not competing with RO systems except in Jeddah where it is in the second place before RO-Wind and this is mainly because of the low average wind speed and relatively higher solar insolation in Jeddah. Optimum location selection for implementing RO-Wind is Dhahran. For RO-PV and MED-Solar, Jeddah and Yanbu are very close to each other and they are the optimum selection. Overall combination-location optimum is RO-Wind in Dhahran.

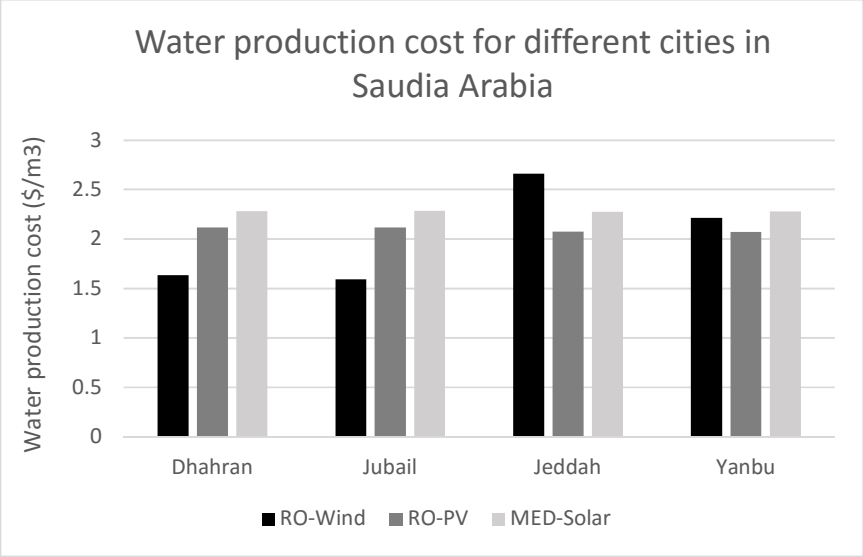

Figure 44: Water production cost by the three systems for different cities in Saudi Arabia.

The obtained desalination water costs are comparable to the values reported in literature. (Koroneos, et al., 2007) reported the water cost for RO-Wind and RO-PV as 1.61 and 2.99 $/m^3$, respectively, for plant capacity of 500 m^3 per day. The results were obtained for a location where average wind speed is 7.5 m/s and average solar irradiation is 5 kWh/day/m^2. (Thomson & Infield, 2002) estimated the cost of battery-less RO-PV system as 2.5 $/$m^3$ in Massawa, Eritrea. Massawa has an average solar irradiation of 5.47 kWh/day/m^2. The system was a demonstration setup to produce only 3 m^3/day. Overall, these results are close to the obtained costs with some deviation. This deviation is mainly caused by one or more of the following reasons:

1. Variation of renewable resources data between the proposed cities and cities in the literature.
2. Systems capacities and feed water concentration.
3. Technical specification of the wind turbines, PV panels, RO modules and others.
4. Time dependence of equipment's cost.

Ministry of Environment, Water and Agriculture has reported water cost in (Ministry of Environment, Water and Agriculture, 2016). Reported water cost is 3.33 $/$m^3$ (12.5 SR/m^3). This cost includes desalination and transportation of water.

5.5 Software interface developed in EES

A simplified diagram window interface is developed using the software package EES. The interface simplifies the usage of the code and reduce it to only limited inputs and outputs and eliminate the dealing with lengthy complicated equations and functions. The diagram window is developed using the available tools embedded in EES software package. Although it does not show the details of the result but user can find them easily using software icons.

The interface contains two columns, one for inputs and the other for outputs. Print screen of the interface is shown in Figure 45. The inputs include the city, daily water demand, feed water concentration and safety factor. A drop-list of cities across the kingdom which contain existing desalination plants, where renewable data and geographical location are stored, is used. The drop-list is shown in Figure 46. If another city rather than the listed is to be analyzed, user may use the option “User defined” and enter the values of latitude and longitude of the city. Also the renewable resources including solar irradiation, wind speed and ambient temperature need to be entered as described.

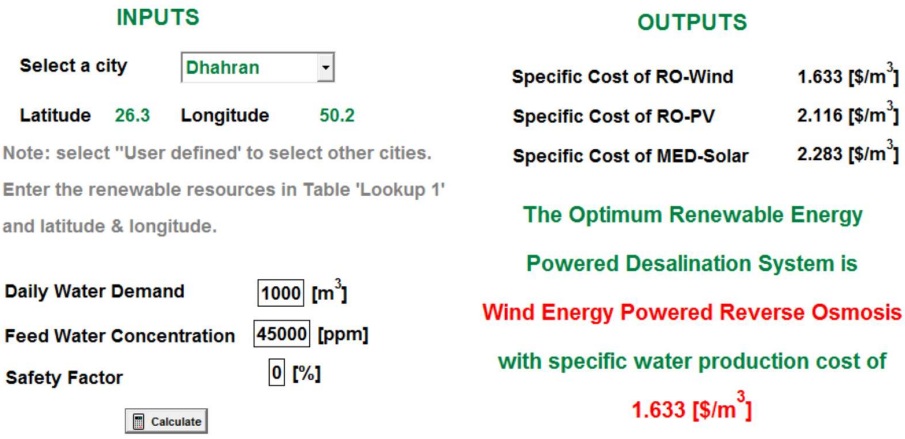

Figure 45: REDS code interface using EES software

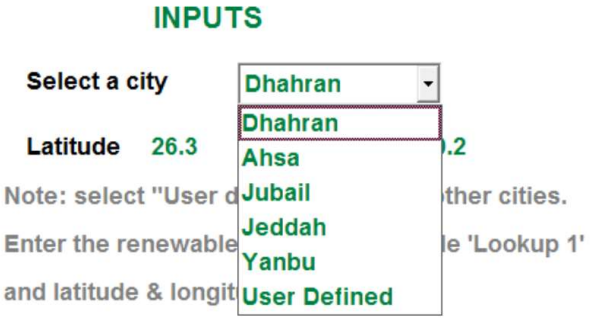

Figure 46: Select city drop list

CONCLUSION

We have presented a thermo-economic methodology for selecting the most cost-effective renewable energy powered desalination system given a geographical location, based on the weather data and required fresh water demand. The methodology has been formulated based on the common published models of renewable energy and desalination subsystems. In order to facilitate the use of this methodology, we have implemented it in EES software and used the code to simulate several practical cases.

For the case of Dhahran, Saudi Arabia, the method predicted that an RO-Wind system produced desalinated water at a cost of \$1.366/m^3 for a daily demand of 1,000 m^3. This was in favor of an RO-PV and MED-Solar systems with costs of \$2.119/m^3.and \$2.282/m^3, respectively.

For RO-Wind and RO-PV, our implementation uses water storage as a method to insure availability of water at any time. This choice is more cost effective, more environmentally friendly and in line with our primary goal of water production, if compared to energy storage using batteries. This implementation produces 100% renewable desalination system. Main reason of the difference between costs of RO-PV and RO-Wind is the larger power and desalination systems required in RO-PV.

For MED-Solar thermal, three configurations were discussed based on the value of the design solar irradiation. Solar field size, and solar share as a result, increases as

design solar irradiation decreases. For Dhahran, renewable share is limited to 24.4%, 37.5% and 43.3% for the values of I_{Design} equal to 991.8, 464.3 and 232.2 W/m2, respectively. MED-Solar is less sensitive to feed water concentration than RO-Wind and RO-PV.

Optimum location selection for implementing RO-Wind is Dhahran. For RO-PV and MED-Solar, Jeddah and Yanbu are very close to each other and they are the optimum selection. Overall combination-location optimum is RO-Wind in Dhahran.

It is highly recommended to extend the work to contain all promising combinations at different configurations.

APPENDIX

Renewable resources data, including monthly daily average solar insolation, monthly daily average wind speed and monthly daily average mean temperature, for four cities in the kingdom of Saudi Arabia. The cities are Dhahran, Jubail, Jeddah and Yanbu. Data are obtained from RETScreen software provided by Natural Resources Canada and NASA Langley Research Center Atmospheric Science Data Center Surface meteorological and Solar Energy (SSE) web portal.

Data of solar insolation and temperature are averaged for a period of 22 years (from July 1983 to June 2005). However, wind speed data are averaged for a period of 10 years (from July 1983 to June 1993).

Table A 1: Monthly average weather data for Dhahran, Saudi Arabia

Month	Insolation ($kWh/m^2/day$)	Wind Speed (m/s)	Mean temperature (°C)
January	3.57	4.2	15.3
February	4.42	4.6	16.8
March	5.13	4.7	20.3
April	6.03	4.6	25.8
May	7.03	4.9	31.6
June	7.73	5.3	34.7
July	7.26	4.7	35.9
August	6.97	4.2	35.3
September	6.45	3.9	32.4
October	5.33	3.7	28.5
November	4	4.1	22.7
December	3.28	4.2	17.5

Table A 2: Monthly average weather data for Jubail, Saudi Arabia

Month	Insolation ($kWh/m^2/day$)	Wind Speed (m/s)	Mean temperature (°C)
January	3.54	4.4	17.1
February	4.48	4.9	18
March	5.16	4.8	20.7
April	5.84	4.5	25.6
May	6.87	5.1	31
June	7.7	5.5	34.4
July	7.35	4.6	36.1
August	7.04	4.6	36
September	6.45	4.2	33.4
October	5.26	3.9	29.4
November	3.93	4.1	24.3
December	3.29	4.4	19.5

Table A 3: Monthly average weather data for Jeddah, Saudi Arabia

Month	Insolation ($kWh/m^2/day$)	Wind Speed (m/s)	Mean temperature (°C)
January	4.53	3.7	23
February	5.32	3.9	23.1
March	6.18	4	24.9
April	6.88	3.8	27.8
May	7.17	3.7	30.1
June	7.12	3.8	31
July	7.04	3.6	32.5
August	6.53	3.7	32.5
September	6.17	3.4	31.4
October	5.56	2.9	29.7
November	4.6	3.1	27.2
December	4.15	3.5	24.7

Table A 4: Monthly average weather data for Yanbu, Saudi Arabia

Month	Insolation ($kWh/m^2/day$)	Wind Speed (m/s)	Mean temperature (°C)
January	4.36	3.2	20.6
February	5.28	3.5	21
March	6.04	3.8	23.6
April	6.73	3.7	27.4
May	7.02	4.1	30.6
June	7.49	4.6	32.1
July	7.3	4.6	32.7
August	6.7	4.5	32.9
September	6.1	4	32.2
October	5.38	3.3	29.7
November	4.37	3.1	25.7
December	4.02	3	22.3

REFERENCES

Abdul-Fattah, A., 1986. Selection of solar desalination system for supply of water in remote arid zones. *Desalination,* 60(2), p. 165–189.

Ahmad, N., Sheikh, A. K., Gandhidasan, P. & Elshafie, M., 2015. Modeling, simulation and performance evaluation of a community scale PVRO water desalination system operated by fixed and tracking PV panels: A case study for Dhahran city, Saudi Arabia. *Renewable Energy,* March , Volume 75, p. 433–447.

Ahmad, N., Sheikh, A. K., Gandhidasan, P. & Elshafie, M., 2015. Modeling, simulation and performance evaluation of a community scale PVRO water desalination system operated by fixed and tracking PV panels: A case study for Dhahran city, Saudi Arabia. *Renewable Energy,* Volume 75, pp. 433-447.

Ali, M. T., Fath, H. E. & Armstrong, P. R., 2011. A comprehensive techno-economical review of indirect solar desalination. *Renewable and Sustainable Energy Reviews,* October , 15(8), p. 4187–4199.

Al-Karaghouli, A. & Kazmerski, L. L., 2013. Energy consumption and water production cost of conventional and renewable-energy-powered desalination processes. *RenewableandSustainableEnergyReviews,* August, Volume 24, p. 343–356.

Al-Karaghouli, A., Renne, D. & Kazmerski, L. L., 2009. Solar and wind opportunities for water desalination in the Arab regions. *Renewable and Sustainable Energy Reviews,* December , 13(9), p. 2397–2407.

Chauhan, A. & Saini, R., 2014. A review on Integrated Renewable Energy System based power generation for stand-alone applications: Configurations, storage options, sizing methodologies and control. *Renewable and Sustainable Energy Reviews,* October , Volume 38, p. 99–120.

Deshmukh, M. & Deshmukh, S., 2008. Modeling of hybrid renewable energy systems. *Renewable and Sustainable Energy Reviews,* January , 12(1), p. 235–249.

Duffie, J. & Beckman, W., 2006. *Solar Engineering of Thermal Processes.* s.l.:John Wiley and Sons.

El-Dessouky, H. T. & Ettouney, H. M., 2002 . *Fundamentals of Salt Water Desalination.* s.l.:Elsevier.

El-Dessouky, H. T., Ettouney, H. M. & Mandani, F., 2000. Performance of parallel feed multiple effect evaporation system for seawater desalination. *Applied Thermal Engineering,* December, 20(17), p. 1679–1706.

Elhadidy, M. & Shaahid, S., 1999. Feasibility of hybrid (wind + solar) power systems for Dhahran, Saudi Arabia. *Renewable Energy,* January–April , 16(1-4), p. 970–976.

Elhadidy, M. & Shaahid, S., 2005. Decentralized/stand-alone hybrid Wind–Diesel power systems to meet residential loads of hot coastal regions. *Energy Conversion and Management,* 46(15-16), p. 2501–2513.

Elhadidy, M. & Shaahid, S., 2007. Wind resource assessment of eastern coastal region of Saudi Arabia. *Desalination,* April , 209(1–3), p. 199–208.

Eltawil, M. A., Zhengming, Z. & Yuan, L., 2009. A review of renewable energy technologies integrated with desalination systems. *Renewable and Sustainable Energy Reviews,* December , 13(9), p. 2245–2262.

Ettouney, H., 2004. Visual basic computer package for thermal and membrane desalination processes. *Desalination,* 15 August , Volume 165, p. 393–408.

Forristall, R., 2003. *Heat transfer analysis and modeling of a parabolic trough solar receiver implemented in Engineering Equations Solver,* Golden: National Renewable Energy Laboratory.

Ghaffoura, N., Bundschuhb, J., Mahmoudic, H. & Goosend, M. F., 2015. Renewable energy-driven desalination technologies: A comprehensive review on challenges and potential applications of integrated systems. *Desalination,* 15 January , Volume 356, p. 94–114.

Ghaffour, N., Missimer, T. M. & Amy, G. L., 2013. Technical review and evaluation of the economics of water desalination: Current and future challenges for better water supply sustainability. *Desalination,* 15 January , Volume 309, p. 197–207.

Gholinejad, M., Bakhtiari, A. & Bidi, M., 2016. Effects of tracking modes on the performance of a solar MED plant. *Desalination,* Volume 380, pp. 29-42.

Groumpos, P. & Papageorgiou, G., 1987. An optimal sizing method for stand-alone photovoltaic power systems. *Solar Energy,* 38(5), p. 341–351.

Gude, V. G., Nirmalakhandan, N. & Deng, S., 2010. Renewable and sustainable approaches for desalination. *Renewable and Sustainable Energy Reviews,* December , 14(9), p. 2641–2654.

Habib, M., Said, S., El-Hadidy, M. & Al-Zaharna, I., 1999. Optimization procedure of a hybrid photovoltaic wind energy system. *Energy,* November, 24(11), p. 919–929.

Habib, M., Said, S., El-Hadidy, M. & Al-Zaharna, I., 1999. Optimization procedure of a hybrid photovoltaic wind energy system. *Energy,* 24(11), p. 919–929.

Kalogirou, S. A., 2005. Seawater desalination using renewable energy sources. *Progress in Energy and Combustion Science,* 31(3), p. 242–281.

Karagiannis, I. C. & Soldatos, P. G., 2008. Water desalination cost literature: review and assessment. *Desalination,* 1 March , 223(1-3), p. 448–456.

Koroneos, C., Dompros, A. & Roumbas, G., 2007. Renewable energy driven desalination systems modelling. *Journal of Cleaner Production,* 15(5), p. 449–464.

Malek, A., Hawlader, M. & Ho, J., 1996. Design and economics of RO seawater desalination. *Desalination,* Volume 105, pp. 245-261.

Ma, Q. & Lu, H., 2011. Wind energy technologies integrated with desalination systems: Review and state-of-the-art. *Desalination,* 15 August , 277(1-3), p. 274–280.

Ministry of Environment, Water and Agriculture, 2016. *Water and Electricity Facts in Saudi Arabia.* [Online]
Available at: http://www.mowe.gov.sa/Arabic/NewRates.pdf
[Accessed 18 12 2016].

Miranda, M. S. & Infield, D., 2003. A wind-powered seawater reverse-osmosis system without batteries. *Desalination,* 10 February , 153(1-3), p. 9–16.

Mohamed, E. S. & Papadakis, G., 2004. Design, simulation and economic analysis of a stand-alone reverse osmosis desalination unit powered by wind turbines and photovoltaics. *Desalination,* 25 March , 164(1), p. 87–97.

Mokheimer, E. M., Sahin, A. Z., Al-Sharafi, A. & Ali, A. I., 2013. Modeling and optimization of hybrid wind–solar-powered reverse osmosis water desalination system in Saudi Arabia. *Energy Conversion and Management,* Volume 75, p. 86–97.

Nafey, A., Fath, H. & Mabrouk, A., 2006. A new visual package for design and simulation of desalination processes. *Desalination,* 10 June, 194(1-3), p. 281–296.

Nafey, A., Fath, H. & Mabrouk, A., 2008. Thermoeconomic design of a multi-effect evaporation mechanical vapor compression (MEE–MVC) desalination process. *Desalination,* Volume 230, p. 1–15.

Nafey, A. & Sharaf, M., 2010. Combined solar organic Rankine cycle with reverse osmosis desalination process: Energy, exergy, and cost evaluations. *Renewable Energy,* November , 35(11), p. 2571–2580.

Palenzuela, P., Alarcon-Padilla, D. C. & Zaragoza, G., 2015. *Concentrating Solar Power and Desalination Plants.* s.l.:Springer.

Peñate, B. & García-Rodríguez, L., 2012. Seawater reverse osmosis desalination driven by a solar Organic Rankine Cycle: Design and technology assessment for medium capacity range. *Desalination,* 4 January , Volume 284, p. 86–91.

Perz, E. W. & Bergmann, S., 2007. A simulation environment for the techno-economic performance prediction of water and power cogeneration systems using renewable and fossil energy sources. *Desalination,* 5 February , 203(1-3), p. 337–345.

Rheinländer, J., Perz, E. W. & Goebel, O., 2003. Performance simulation of integrated water and power systems — software tools IPSEpro and RESYSpro for technical, economic and ecological analysis. *Desalination,* 1 August, 157(1-3), p. 57–64.

Shaahid, S. & Elhadidy, M., 2003. Opportunities for utilization of stand-alone hybrid (photovoltaic + diesel + battery) power systems in hot climates. *Renewable Energy,* September, 28(11), p. 1741–1753.

Sharaf, M., Nafey, A. & García-Rodríguez, L., 2011. Exergy and thermo-economic analyses of a combined solar organic cycle with multi effect distillation (MED) desalination process. *Desalination,* Volume 272, pp. 135-147.

Thomson, M. & Infield, D., 2002. A photovoltaic-powered seawater reverse-osmosis system without batteries. *Desalination,* Volume 153, pp. 1-8.

Yang, H., Wei, Z. & Chengzhi, L., 2009. Optimal design and techno-economic analysis of a hybrid solar–wind power generation system. *Applied Energy,* February , 86(2), p. 163–169.

Zhou, W. et al., 2010. Current status of research on optimum sizing of stand-alone hybrid solar–wind power generation systems. *Applied Energy,* February , 87(2), p. 380–389.

Vitae

Name :Ahmad Hussain Al-Jabr

Nationality :Saudi

Date of Birth :4/24/1987

Email :aljabrah@kfupm.edu.sa; aljabraha@gmail.com

Address :King Fahd University of Petroleum and Minerals (KFUPM), Dhahran, Kingdom of Saudi Arabia

Academic Background :

Master of Science in Mechanical Engineering: King Fahd University of Petroleum and Minerals (KFUPM), Dhahran, Saudi Arabia, 2016

Bachelor of Science Mechanical Engineering: King Fahd University of Petroleum and Minerals (KFUPM), Dhahran, Saudi Arabia, 2010